JOC The Journal of Organic Chemistry

Article

pubs.acs.org/joc

Four- and Five-Component Syntheses and Photophysical Properties of Emission Solvatochromic 3-Aminovinylquinoxalines

Charlotte F. Gers-Panther,[†] Henry Fischer,[‡] Jan Nordmann,[†] Theresa Seiler,[†] Thomas Behnke,[‡] Christian Würth,[‡] Walter Frank,[§] Ute Resch-Genger,*[,‡] and Thomas J. J. Müller*[,†]

[†]Institut für Organische Chemie und Makromolekulare Chemie, Heinrich-Heine-Universität Düsseldorf, Universitätsstrasse 1, D-40225 Düsseldorf, Germany

[‡]Bundesanstalt für Materialforschung und -prüfung (BAM), Richard-Willstätter-Strasse 11, D-12489 Berlin, Germany

[§]Institut für Anorganische Chemie und Strukturchemie, Heinrich-Heine-Universität Düsseldorf, Universitätsstrasse 1, D-40225 Düsseldorf, Germany

Supporting Information

ABSTRACT: 3-Aminovinylquinoxalines are readily accessible from (hetero)aryl glyoxylic acids or heterocyclic π-nucleophiles by consecutive four- and five-component syntheses in the sense of an activation-alkynylation-cyclocondensation-addition sequence or glyoxylation-alkynylation-cyclocondensation-addition sequence in good yields. The title compounds are highly fluorescent with pronounced emission solvatochromicity and protochromic fluorescence quenching. Time-resolved fluorescence spectroscopy furnishes radiative and nonradiative fluorescence decay rates in various solvent polarities. The electronic structure is corroborated by DFT and TD-DFT calculations rationalizing the observed spectroscopic effects.

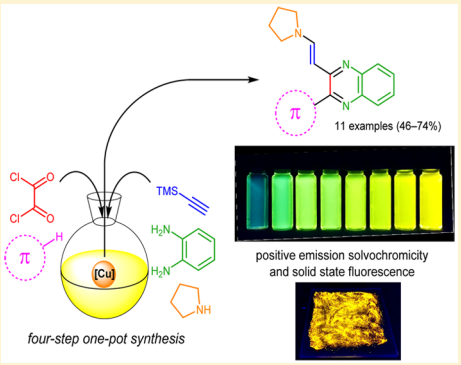

INTRODUCTION

In the past decades, functional organic compounds have increasingly received interest in the context of materials and life sciences.[1] Besides carbon-rich π-systems and organic polymers, small organic molecules have aroused attention in a variety of fields, ranging from organic electronics[2] (OFET, OLED, and DSSC)[3] to imaging and sensing applications in biochemical,[4] environmental, and clinical applications.[5] In this area, fluorescence detection adopts a central position, offering many advantages over other competing methods of detection. This is related to the fact, that fluorescence is a multiparameter technique requiring comparatively simple and inexpensive instrumentation and offering a unique sensitivity down to the single molecule or particle level.[6] Fluorescence detection is closely linked to fluorescent labels and probes responding to physicochemical or chemical quantities and changes of their local environment, such as polarity, viscosity, or proticity/hydrogen bonding, with changes in the spectral position and/or intensity of their absorption and emission bands.[7] This includes also the presence and concentration of biologically or diagnostically relevant ionic or neutral analytes, such as protons or molecular oxygen. For example, polarity sensing is often applied in molecular cell biological and biochemical studies, i.e., for monitoring folding and unfolding processes of proteins or for estimating the polarity of protein binding sites.[4] Favorable for such applications are fluorophores, which display different emission colors depending on the polarity of the surrounding media.[8] Such compounds are generally highly polar and experience a significant change of their dipole moment upon excitation from S_0 to S_1.[9] This by eye-sight observable phenomenon is called solvatochromism,[10] and can occur in absorption and/or emission.[11] Such properties are commonly obtained by the introduction of electron donating and withdrawing moieties to a molecule.

The increasing demand for tailor-made fluorophores requires constantly novel structural motifs and innovative synthetic approaches. For establishing reliable structure−property relationships of the photophysical behavior of novel compound classes, often libraries are particularly valuable. In this context, the concepts of combinatorial chemistry[12] and diversity-oriented synthesis[13] are highly advantageous, since highly diverse products[14] can be readily attained through variation of the different starting materials. In particular, multicomponent reactions (MCR)[15] and one-pot strategies adopt a central role, since they combine beneficial economic and ecological factors, such as higher resource efficiency and lower waste production compared to the classical multistep synthesis. In the past decades, MCR regularly found application in the synthesis of natural products[16] and pharmaceutically interesting compounds[17] and more recently, they have become a powerful tool for fluorophore design.[18]

Received: October 25, 2016
Published: December 15, 2016

DOI: 10.1021/acs.joc.6b02581
J. Org. Chem. 2017, 82, 567−578

In recent years, the quinoxaline core was regularly incorporated as an electron acceptor in push−pull systems and intramolecular charge-transfer complexes (ICT)[19] owing to their peculiar electronic nature. The presence of two nitrogen atoms leads to a highly electron deficient π-system.[20] A large number of these compounds are luminescent and their high polarity expresses itself by pronounced solvatochromic shifts of the emission bands. Only recently, we[21] and Zhang's group[22] described the synthesis of emission-solvatochromic indole-substituted quinoxaline derivatives. Another solvatochromic quinoxaline-based push−pull system was reported by Kudo et al. which was employed to classify the binding-site polarity of bovine serum albumin[23] and even shows site-dependent fluorescence in HEp-2 cells.[24] The electron-withdrawing character of quinoxalines has also led to their incorporation into chromophores for dye-sensitized solar cells.[25]

In general, quinoxalines are easily accessible by cyclo-condensation of 1,2-diaminoarenes and 1,2-dicarbonyl compounds,[26] the so-called Hinsberg reaction.[27] Interestingly, quinoxalines are hardly found in natural products, nevertheless many synthetic derivatives possess biological activities[28] with some being accounted to the best-selling drugs containing six-membered heterocycles.[29] Our group has recently reported two complementary diversity-oriented one-pot approaches for the synthesis of quinoxaline derivatives through intermediary reactive ynediones (Scheme 1).[21] In the first step, both methods

Scheme 1. Four-Component (GACC Sequence) and Three-Component (AACC Sequence) One-Pot Syntheses of Ethynylquinoxalines 6

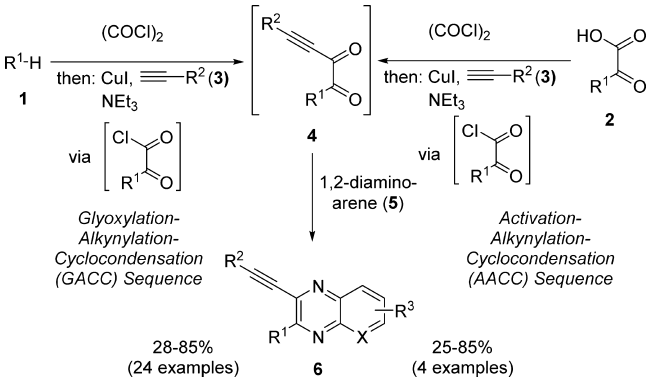

generate glyoxylic acid chlorides starting either from a π-nucleophile **1** or a glyoxylic acid **2**, which are subsequently converted into ynediones **4** through a copper-catalyzed Stephens-Castro alkynylation.[30] The formed ynediones are subsequently reacted with 1,2-diaminoarenes to produce the desired quinoxalines **6**, leaving the triple bond untouched. The ethynylquinoxalines **6** are fluorescent and display pronounced emission solvatochromism, which was ascribed to the push−pull character between the electron-rich heterocyclic substituent R^1 in 2-position and the electron deficient quinoxaline ring.

These beneficial electronic properties should be amplified by increasing the push−pull character through the introduction of an additional, even stronger donor substituent. Inspired by the universal functionality of triple bonds in synthetic organic chemistry, we became intrigued to employ the alkyne functionality for subsequent transformations, eventually in a one-pot scenario. Ethynylquinoxalines should be susceptible to nitrogen nucleophiles, in analogy to alkynones[31] or classical Michael systems (Scheme 2), caused by the electron-withdrawing character of the quinoxaline core, furnishing enamine-

Scheme 2. Electrophilicity Mapping of Ethynylquinoxalines

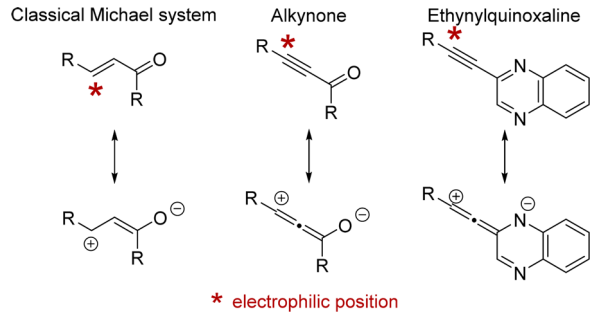

type structures.[32] Similar strategies were also employed in the synthesis of various heterocyclic scaffolds through an intramolecular ring closure.[32b,33]

The addition of nitrogen-based nucleophiles to the triple bond would ultimately result in a second strongly electron-donating substituent on the quinoxaline core, namely an aminovinyl group.[34] Aminoquinoxaline-based push−pull systems had previously been a subject of photophysical studies, however, both units were either ligated by a phenyl[35] or styryl[19b] linker. Here, we report four- and five-component syntheses of novel 3-aminovinylquinoxalines, their structures and first studies of their photophysical properties and their electronic structures.

RESULTS AND DISCUSSION

Synthesis. For studying the addition of secondary amines to the triple bond, a terminally unsubstituted ethynylquinoxaline and pyrrolidine were chosen as model substrates to ensure a high reactivity. Starting from TMS-ethynylquinoxaline **6a**,[21] the terminal alkyne was quantitatively obtained by cleaving of the TMS group in the presence of KF and methanol.[36] Compound **7a** can be easily transformed into the desired 3-amino-vinylquinoxaline **9a** upon addition of pyrrolidine (**8a**) in a mixture of THF and MeOH as the solvent system (Scheme 3). Much to our delight, the combination of pyrrolidine and methanol generated sufficiently basic conditions to cleave the TMS group in situ and, therefore, enabled a domino desilylation-addition-sequence to obtain the corresponding 3-pyrrolidinovi-

Scheme 3. Two-Step and Domino Access to 3-Pyrrolidinovinylquinoxaline 9a from TMS-ethynylquinoxaline 6a

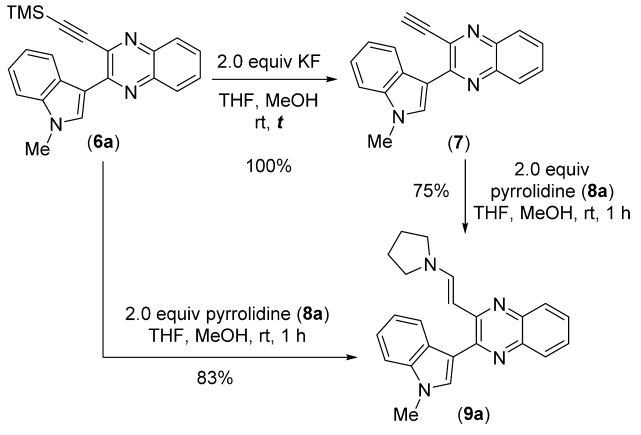

DOI: 10.1021/acs.joc.6b02581
J. Org. Chem. 2017, 82, 567−578

Table 1. One-Pot Four-Step Synthesis of 3-Aminovinylquinoxalines 9

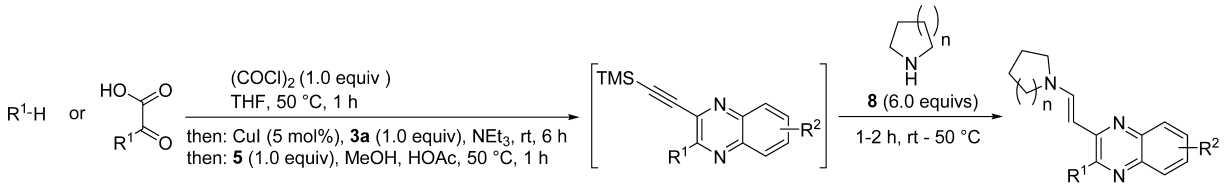

1 **2** **6** **9**

Entry	Starting material **1** or **2**	1,2-Diamino arene **5**	3-Ethynylquinoxaline **6**[a]	Secondary amine **8**	3-Aminovinylquinoxaline **9** (yield)
1	1-methylindole (**1a**)	*ortho*-phenylene diamine (**5a**)	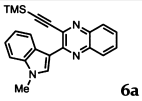 **6a** (77%)	pyrrolidine (**8a**)	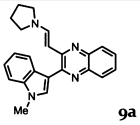 **9a** (73%)[b]
2	1-methylpyrrole (**1b**)	**5a**	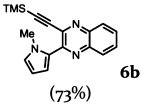 **6b** (73%)	**8a**	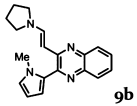 **9b** (74%)[b]
3	2-methoxythiophene (**1c**)	**5a**	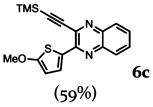 **6c** (59%)	**8a**	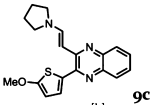 **9c** (60%)[b]
4	phenyl glyoxylic acid (**2a**)	**5a**	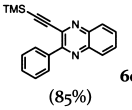 **6d** (85%)	**8a**	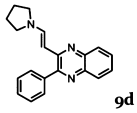 **9d** (57%)[b]
5	2-thiophene glyoxylic acid (**2b**)	**5a**	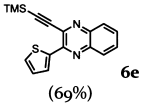 **6e** (69%)	**8a**	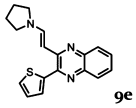 **9e** (69%)[b]
6	1-methylindole (**1a**)	1,2-diamino 4,5-dichloro benzene (**5b**)	-	**8a**	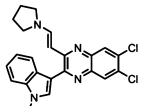 **9f** (68%)[c]
7	phenyl glyoxylic acid (**2a**)	**5b**	-	**8a**	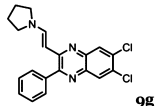 **9g** (52%)[c]
8	2-thiophene glyoxylic acid (**2b**)	**5b**	-	**8a**	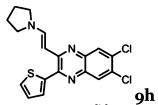 **9h** (65%)[b]
9	2-thiophene glyoxylic acid (**2b**)	2,3-diamino naphtha-lene (**5c**)	-	**8a**	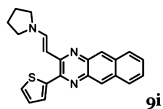 **9i** (61%)[b]
10	phenyl glyoxylic acid (**2a**)	**5a**	-	piperidine (**8b**)	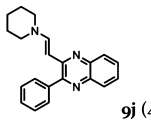 **9j** (46%)[d]

[a]Yield of the intermediary 3-ethynylquinoxaline **6**, if isolated. [b]Reaction conditions for the amine addition step: 1 h, rt. [c]Reaction conditions for the amine addition step: 1 h, 50 °C. [d]Reaction conditions for the amine addition step: 2 h, 50 °C.

nylquinoxaline **9a** exceeding the combined yields of the stepwise process.

With this simple transformation of ethynylquinoxaline **6a** to the corresponding 3-pyrrolidinovinylquinoxaline **9a** in hand, we reasoned that a concatenation of the previously reported one-pot synthesis of ethynylquinoxalines should furnish an efficient access to 3-aminovinylquinoxalines **9** in a consecutive four component or five component fashion. The particular challenge in designing this sequence is the combination of reaction steps proceeding in alternating pH regions, i.e., (1) glyoxylation and

DOI: 10.1021/acs.joc.6b02581
J. Org. Chem. 2017, 82, 567−578

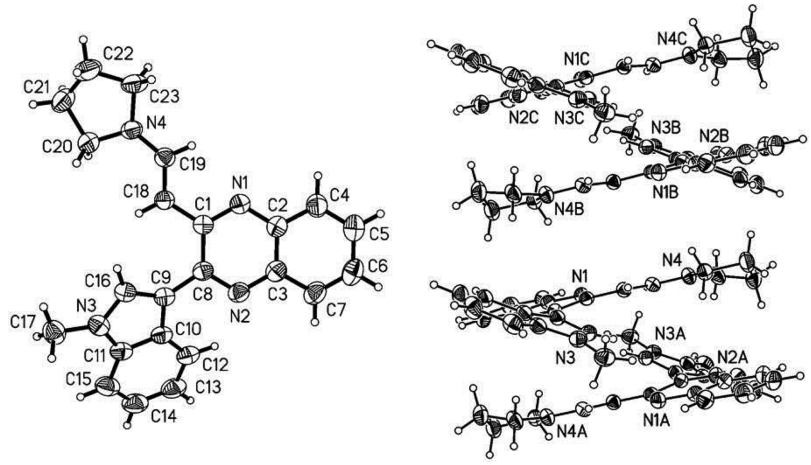

Figure 1. Left: Diagram of the molecular structure of **9a** in the crystal. Right: Packing of molecules to columns. Displacement ellipsoids are drawn at the 30% probability level. Selected torsion angle: C1−C8−C9−C16−35.7(2).

activation (acidic); (2) alkynylation (basic); (3) cyclocondensation (acidic); (4) desilylation and amine addition (basic). This can result in a considerable salt formation as byproducts, which often hamper the smooth course of a reaction. Therefore, we set out to optimize the envisaged process with a special focus on consequently minimizing the amounts of additives, such as triethylamine and acetic acid (see Supporting Information, Tables S1 and S2). As a result of the optimization study of the one-pot glyoxylation-alkynylation-cyclocondensation synthesis of **6a** (see Supporting Information, Table S2) the concatenation with the terminal pyrrolidine addition was probed and optimized (see Supporting Information, Table S3). Most importantly a 6-fold excess of pyrrolidine (**8a**) in conjunction with a chromatographic purification on basic alumina with dichloromethane as an eluent proved to furnish a yield of 76% of 3-pyrrolidinovinylquinoxaline **9a** for the four step one-pot synthesis.

These optimized conditions for preparation and isolation were then applied to all four- and five-component syntheses of 3-aminovinylquinoxalines **9** starting from either π-nucleophiles **1** or glyoxylic acids **2** (Table 1). Much to our delight, the sequence represents a highly modular approach to a library of the desired compounds mostly in excellent yields. The corresponding 3-aminovinylquinoxalines arising from 3-(aryl)ethynylquinoxalines were found to hydrolyze upon flash chromatography. It is noteworthy to mention that, with exception of the secondary amine **8**, all components are employed in strictly equimolecular ratios. Applying both reaction sequences allows the introduction of different heterocyclic moieties to the quinoxaline core (Table 1, entries 1−3, 5, 6, 8, 9) as well as a phenyl ring (Table 1, entries 4, 7, 10) with generally excellent yields. Comparing the yields of these four-step sequences with the yields of the three-step 3-ethynylquinoxaline formation[30a] reveals that the terminal amine addition proceeds almost quantitatively, except for employing phenylglyoxylic acid as a starting material (Table 1, entry 4). 1,2-Diamino-4,5-dichlorobenzene (**5b**) and 2,3-diaminonaphthalene (**5c**) can be also utilized in the synthesis of 3-aminovinylquinoxalines, although the yields are slightly lower (Table 4, entries 6−9). Piperidine (**8b**) as a secondary amine furnishes the 3-piperidinovinylquinoxaline **9j** (Table 1, entry 10). Acyclic secondary amines were not employed in the one-pot sequence. They were found to react sluggishly in the single-step reaction and the products partly hydrolyzed upon chromatographic purification. Their isolation by crystallization was not successful. Taking into account that six new bonds are formed in a consecutive four-step fashion the average yields per bond forming step accounts to 88−95%.

The proposed structures of the 3-aminovinylquinoxalines **9** were unambiguously supported with ^{1}H and ^{13}C NMR spectroscopy, mass spectrometry, IR spectroscopy, and combustion analysis. It is noteworthy that all derivatives were exclusively formed as single diastereomers. The vicinal coupling constants for the vinyl protons lie in the range of 12.6 to 12.8, suggesting the formation of the thermodynamically favored (*E*)-configuration for the double bond. The structures of compounds **9** were additionally corroborated by X-ray crystal structure determination of compound **9a** (Figure 1).[37]

PHOTOPHYSICAL PROPERTIES—SPECTROSCOPIC STUDIES AND CALCULATIONS

Solvatochromism. The solvatochromism of our four selected 3-aminovinylquinoxalines **9a**−**9d** was subsequently thoroughly studied by absorption as well as steady state and time-resolved fluorescence spectroscopy in nine solvents of different polarity to confirm the theoretical assumptions, assessing absorption and fluorescence maxima, fluorescence quantum yields Φ, and fluorescence lifetimes τ. Figure 2 compares the absorption and emission spectra of **9a**−**9d** in acetonitrile. In the UV region below 400 nm, all dyes show a unique absorption pattern. The order of the longest wavelength absorption maxima ($\lambda_{max(abs)}$) of **9a**−**9d** is as follows: **9d** (438 nm), **9a** (440 nm), **9b** (445 nm), and **9c** (456 nm), respectively. This trend is also reflected by the emission spectra in acetonitrile

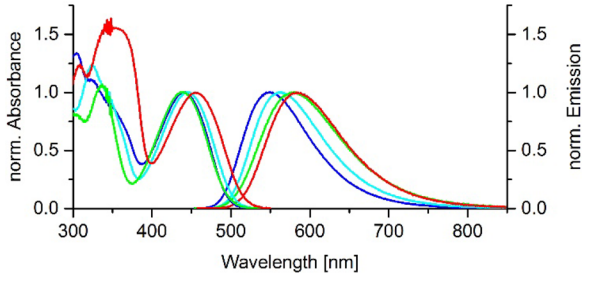

Figure 2. Normalized absorption (550 nm and below) and emission spectra (450 nm and above) of **9a**−**9d** in acetonitrile (**9a**: blue; **9b**: cyan; **9c**: green; **9d**: red).

DOI: 10.1021/acs.joc.6b02581
J. Org. Chem. 2017, 82, 567−578

shown in Figure 2, with the broad shape of these bands underlining the charge transfer (CT) character of this transition.

The influence of the polarity of the surrounding medium on the emission of the 3-aminovinylquinoxalines is shown for **9a** in Figure 3. In nonpolar, aprotic solvents like cyclohexane, the dye's

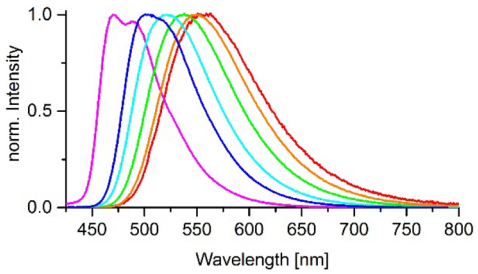

Figure 3. Emission bands of **9a** in solvents of varying polarity and proticity. from left to right: cyclohexane (magenta), toluene (blue), tetrahydrofuran (cyan), acetone (green), acetonitrile (orange), ethanol (red).

emission band, located at ca. 475 nm, reveals a vibronic fine structure. With increasing solvent polarity, this vibronic structure is lost and the emission bands are shifted bathochromically by up to 3291 cm^{-1}. This behavior is typical for CT-operated fluorophores and implies a positive solvatochromism of this family of dyes.

For comparison of the measured spectroscopic and the calculated data, we considered the empirical solvent polarity parameter E_T^N. E_T^N values are correlated to the electronic transition energies of the chromogenic dye pyridinium *N*-phenolate betaine, a well-established polarity probe.[11] The plot of the Stokes shift as a function of E_T^N values reveal the experimentally determined $\Delta\mu$ (see Supporting Information, Figure S2, Table S2).

Additionally, the fluorescence quantum yields Φ and the fluorescence lifetimes τ of dyes **9a**–**9d** were measured in different solvents. The corresponding data are summarized in Table 2. The highest Φ value of 61.1% resulted for **9b** in dichloromethane; with values of 0.6 to 1.2% and 2.2 to 4.8% the lowest Φ are found for all dyes in methanol and ethanol, respectively. As follows from Table 2, dyes **9a**, **9b**, and **9d** are significantly more emissive than dye **9c**, which possesses the smallest torsional angle between the 2-substituent, i.e., the thiophene moiety, and the quinoxaline core. Additionally, the heavy atom effect likely plays a role in the quenching process. The lifetimes τ of the dyes **9a**–**9d** reveal a similar dependence on solvent and dye structure as Φ. In summary, for **9a**–**9d**, Φ and τ increase with increasing solvent polarity up to E_T^N of about 0.3 and then decrease with increasing polarity. The very small values in the most polar, yet also protic solvents ethanol and methanol are ascribed to additional contributions from hydrogen bonding induced fluorescence quenching as observed for many CT-operated fluorophores.

Subsequently, we calculated the radiative and nonradiative rate constants k_r and k_{nr} of the dyes **9a**–**9d** from measured Φ and τ in Table 2 (see also Supporting Information);[38] the resulting rate constants were then plotted as a function of E_T^N as summarized in Figure 4. As shown in Figure 4 (right), k_r decrease with increasing

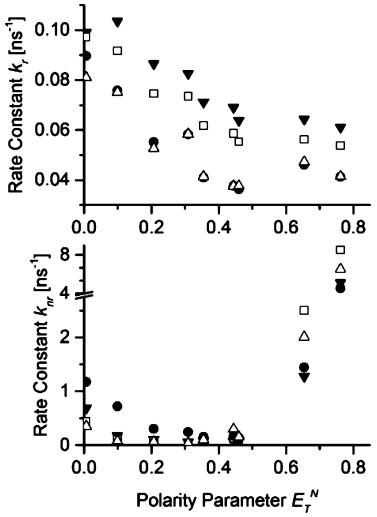

Figure 4. Radiative (top) and nonradiatve (bottom) rate constants plotted against E_T^N. **9a**: triangle downward; **9b**: square; **9c**: circle; **9d**: triangle upward.

solvent polarity for all four dyes up to E_T^N of about 0.3 and then remains more or less constant, whereas k_{nr} of **9a**–**9d** decrease up to E_T^N of about 0.3 and then strongly increases (see Figure 4, left).

High values of k_{nr} in low polarity solvents suggest a radiationless relaxation due to σ bond rotations;[39] such σ bond rotations are possible for the substituents of all quinoxalines studied. The fact that for high E_T^N values, which correspond to the alcohols ethanol and methanol, we see exclusively high values for k_{nr} whereas the size of k_r remains almost constant for $E_T^N > 0.3$ confirms our assumption of fluorescence quenching due to the formation of hydrogen bonds between the hydroxyl groups of the alcohols and the dye molecules.[40,41] This encouraged us to perform protonation studies, thereby also assessing the dyes'

Table 2. Fluorescence Quantum Yields and Lifetimes of the Dyes 9a–9d in Solvents of Different Polarity and Proticity

		9a		9b		9c		9d	
E_T^N	solvent	Φ [%]	τ [ns]	Φ [%]	τ [ns]	Φ [%]	τ [ns]	Φ [%]	τ [ns]
0.762	methanol	1.2	0.19	0.6	0.12	0.9	0.22	0.6	0.15
0.654	ethanol	4.8	0.75	2.2	0.39	3.1	0.67	2.3	0.49
0.460	acetonitrile	43.0	6.75	33.0	5.96	21.0	5.78	19.9	5.28
0.444	DMSO	49.6	7.19	32.5	5.54	18.4	4.88	11.2	2.97
0.355	acetone	45.6	6.42	41.4	6.72	20.9	5.10	28.4	6.88
0.309	dichloromethane	57.9	7.01	61.1	8.33	19.0	3.28	59.8	10.25
0.207	tetrahydofuran	44.4	5.12	49.5	6.61	15.5	2.79	44.5	8.42
0.099	toluene	37.5	3.62	46.9	5.10	9.5	1.25	49.0	6.52
0.006	cyclohexane	12.6	1.27	18.4	1.87	7.2	0.79	18.6	2.30

DOI: 10.1021/acs.joc.6b02581
J. Org. Chem. 2017, 82, 567–578

protonation sites more closely, which are detailed in a separate section.

Calculated Electronic Structure of 3-Aminovinylquinoxalines 9. A deeper rationalization of the photophysical behavior of quinoxalines **9a**–**9d** was sought by elucidating the electronic structure by calculating UV/vis absorption spectra on the DFT level of theory, with a special focus on the origin of the five longest wavelength absorption maxima of each structure. The structures were chosen as a series of compounds with three electron-donating (**9a**–**9c**) and one electron-neutral substituent (**9d**) in position 2 of the quinoxaline core. For this purpose, first the geometries of the ground state structures were optimized using Gaussian09[42] with the B3LYP functional[43] and the Pople 6-311G(d,p) basis set.[44] Since all measurements were recorded in solution, the calculations were carried out using the polarizable continuum model (PCM) applying acetonitrile as a solvent.[45] All minima structures were confirmed by analytical frequency analyses.

The computed equilibrium ground state structure of **9a** matches with the structure obtained from X-ray analyses. The experimentally determined torsional angle between the *N*-methylindole substituent and quinoxaline core is well reproduced by the computations ($\theta_{calc} = -37°$ vs $\theta_{X\text{-}ray} = -36°$).

A closer inspection of the coefficient densities in the Kohn–Sham frontier molecular orbitals of the *N*-pyrrolidinylvinyl **9a**–**9d** reveals that the HOMO coefficient densities are predominantly localized on the quinoxaline ring and the adjacent vinyl moiety, while it is much lower on the substituent in 2-position (Figure 5). The phenyl ring of compound **9d** bears essentially no

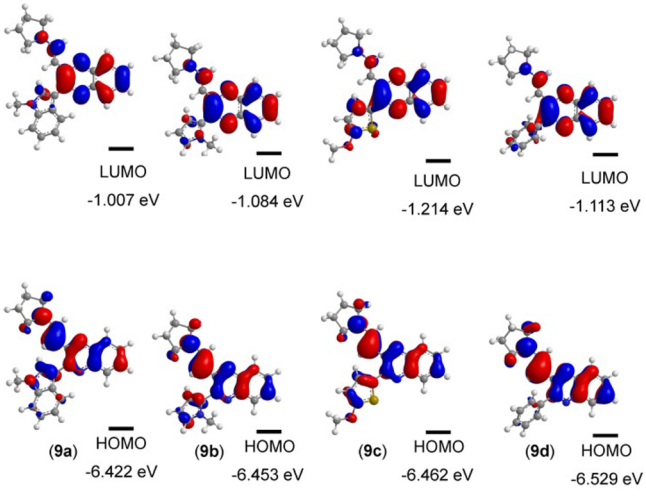

Figure 5. Selected DFT-computed (B3LYP 6-311G(d,p)) Kohn–Sham frontier molecular orbitals of 3-*N*-pyrrolidinylvinylquinoxalines **9a**–**9d**.

coefficient density. Concerning the LUMOs, a quite different picture emerges. In all four derivatives, the coefficient density on the vinyl moiety is much less pronounced, while it is slightly increased on the quinoxaline. This provides a clear hint for the proposed charge transfer (CT) character in the excited state. The effect on the 2-substituent appears to be only minor; while a slightly lower coefficient density is found on the indole and pyrrole moiety, it is enhanced on the thiophene and phenyl ring.

The optimized structures of the 3-aminovinylquinoxalines **9a**–**9d** were subjected to TD-DFT calculations to study the absorption characteristics (Table 3). The hybrid exchange-correlation functional CAM-B3LYP[46] was implemented and a nonequilibrium solvation[47] for the state-specific solvation of the vertical excitation was included.

Expectedly, the longest wavelength absorption bands of all four computed molecules **9a**–**9d** result from HOMO–LUMO transitions. The calculated oscillator strength correlates nicely with the experimentally determined molar decadic extinction coefficients ε underlining the π–π^* character of this transition. Although the experimentally obtained absorption maxima are slightly bathochromically shifted by 756 to 1394 cm^{-1} with respect to the theoretically determined maxima, the trends revealed by theory and experiment are in excellent agreement.

Additionally, the dipole moments μ and the Onsager radius a were calculated (Table 4). The dyes **9a** and **9c** possess the highest dipole moments in the ground state and in the excited state as well, followed by **9d** and **9b**. The experimentally determined $\Delta\mu$ of dyes **9a**–**9d**, although smaller, confirm the trend of the calculated $\Delta\mu$ values, revealing the largest change for **9d** and the smallest effects for **9b** and **9a**.

Table 4. Calculated Values of the Dipole Moments and the Onsager Radius *a* of 9a–9d in Acetonitrile (Using Gaussian09 B3LYP 6-311+ (d,p))

	dipole moment μ [D]			
compound	ground state	excited state (nonrelaxed)	excited state (relaxed)	radius *a*
9a	10.49	16.26	15.34	4.75
9b	5.82	11.92	11.28	4.70
9c	9.77	16.18	15.75	5.00
9d	7.48	14.10	13.43	4.75

Protonation Studies with 3-Aminovinylquinoxalines 9a–9d. In general, quinoxalines are weakly basic, as follows from the pK_a of 0.56 of the parent compound shown in Scheme 4.[26a] Moreover, some quinoxaline-based chromophores display a substantial protochromism upon addition of acids, such as PTSA (*p*-toluene sulfonic acid).[19b,48] The presence of strong acids generally leads to the protonation of a nitrogen atom. Compounds **9c**–**9d** contain three, compounds **9a**–**9b** even four basic nitrogen atoms, which could principally undergo protonation. We therefore reasoned that studies on the protonation behavior of the 3-aminovinylquinoxalines should

Table 3. TD-DFT Calculations (CAM-B3LYP 6-311G(d,p)) of the Absorption Maxima of 3-Aminovinylquinoxalines 9a–9d in Acetonitrile

	experimental $\lambda_{max(abs)}$	calculated $\lambda_{max(abs)}$		
compound	[nm] (ε [$m^{-1}cm^{-1}$])	[nm]	[eV] (oscillator strength)	dominant contributions (%)
9a	440 (17300)	416	2.98039 (0.4081)	HOMO→LUMO (96)
9b	445 (20500)	419	2.95905 (0.3772)	HOMO→LUMO (96)
9c	456 (15300)	441	2.81143 (0.3165)	HOMO→LUMO (96)
9d	438 (16100)	419	2.95905 (0.3741)	HOMO→LUMO (96)

DOI: 10.1021/acs.joc.6b02581
J. Org. Chem. 2017, 82, 567–578

Scheme 4. Mesomeric Forms of the Free Base and Its Conjugated Acid

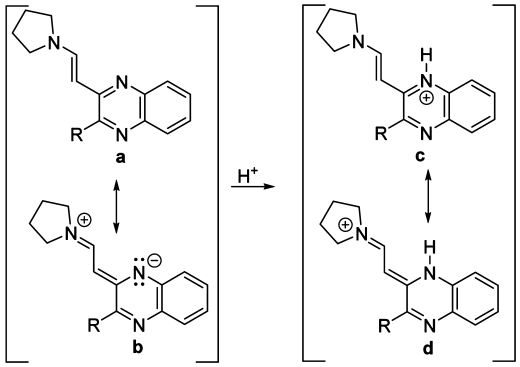

give insights into the reactivity of these quinoxalines. The structural resemblance of the 3-aminovinylquinoxalines to vinamidines[49] suggests the quinoxaline-N1 position as the most probable protonation site, leading to a stabilized vinamidinium ion (Scheme 4).

This assumption is additionally supported by a closer inspection of the pyrrolidine and the double bond signals in the respective ^{1}H and ^{13}C NMR spectra (Table 5). The carbon

Table 5. Comparison of Characteristic ^{1}H and ^{13}C NMR Signals of Free Base 9a and the Corresponding Protonated Species 9a-H^{+}

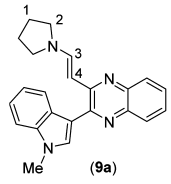

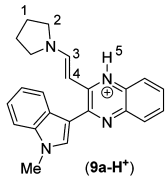

	^{1}H NMR		^{13}C NMR		
Position	**9a**	**9a-H^{+}**	Position	**9a**	**9a-H^{+}**
H1	1.80-1.97 (m, 4 H)	1.95-2.01 (m, 4 H)	*C1*	25.2	24.7 24.8
H2	3.28 (br, 4 H)	3.18 (t, *J* = 5.9 Hz, 2 H) 3.95 (t, *J* = 6.0 Hz, 2 H)	*C2*	49.1	47.6 53.9
H3	8.17 (d, *J* = 12.7 Hz, 1 H)	10.13 (d, *J* = 12.4 Hz, 1 H)	*C3*	143.0	154.8
H4	5.61 (d, *J* = 12.7 Hz, 1 H)	5.68 (d, *J* = 12.6 Hz, 1 H)	*C4*	94.0	89.3
H5	-	14.99-15.10 (br)	-	-	-

nuclei of the pyrrolidine unit of compound **9a** appear as two signals at δ 25.2 and 49.1, while for the protonated form two sets for both signals can be found. While there is only a minor separation of the C1 nuclei (δ 24.7 and 24.8), the signals for C2 considerably differ (δ 47.6 and 53.9). A similar behavior can be observed in the ^{1}H NMR spectrum, however, only for the protons at position 2 (δ 3.18 and 3.95).

These results indicate protonation at the quinoxaline nitrogen atom, which is in close proximity to the aminovinyl moiety. According to the vinamidinium type resonance structure **d** (Scheme 4), the carbon nuclei at positions 1 and 2, respectively, are not magnetically equivalent, which results in the observed signal splitting in both ^{1}H and ^{13}C NMR spectra.

The proposed protonation site as well as the *E*-configuration of compound **9a-H^{+}** was additionally supported by the two-dimensional NOESY spectrum, where significant cross-peaks were found between the *N*-proton and the two ethenyl protons. The combination with the third cross-peak to the neighboring proton of the quinoxaline benzene ring gives evidence for the suggested structure (Scheme 5).

Scheme 5. NOESY Cross-Peaks for Compound 9a-H^{+}

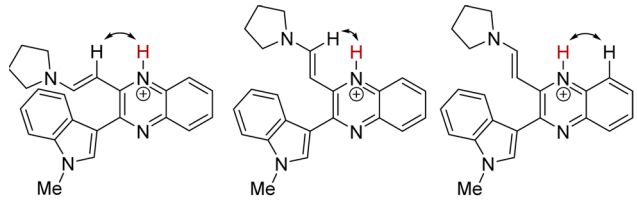

Hints for the proposed protonation site were also obtained from DFT-calculations based on the structure of **9a**. A thermodynamic comparison of four different protonated species **9a-H^{+}** revealed the protonation at the quinoxaline-N1 and N2 positions to be thermodynamically most favorable (Figure 6).

This encouraged us to perform a spectroscopic protonation study representatively for two dyes, here a titration experiment with **9a** and **9d** in a DMSO-water mixture adding different amounts of hydrochloric acid (Figure 7). As summarized in Figure 7, with increasing proton concentration, a bathochromic shift in absorption together with a change in spectral shape and an increase in intensity occurred. These changes in absorption reflect the protonation-induced weakening of the electron donor. The observation of an isosbestic point for both dyes (**9a**: 430 nm; **9d**: 441 nm) underlines the formation of a single protonation product and quantitative 1:1 transformation without side products. From the changes in absorption, the pK_a values were calculated to 4.26 for **9a-H^{+}** and 3.7 for **9d-H^{+}**, respectively. This agrees with the slightly higher electron density at the quinoxaline nitrogen atom found for **9a** compared to **9d** according to the Mulliken charges. The protonation was reversible as revealed by addition of base. As shown in Figure 7, protonation leads to a strong decrease in fluorescence for both dyes, with the protonated species always being nonemissive. This follows from excitation spectra measured for different concentrations of hydrochloric acid which show only the absorption band of the nonprotonated (emissive) species and match with the absorption spectrum of the corresponding dye without hydrochloric acid. A protonation-induced fluorescence quenching has been reported for many CT-operated dyes. This observation agrees well with the hydrogen bonding induced diminution in fluorescence observed in polar protic solvents like ethanol and methanol described in a previous section.

CONCLUSION

Four- and five-component syntheses of 3-aminovinylquinoxalines have been established. The diversity-oriented nature of this

DOI: 10.1021/acs.joc.6b02581
J. Org. Chem. 2017, 82, 567−578

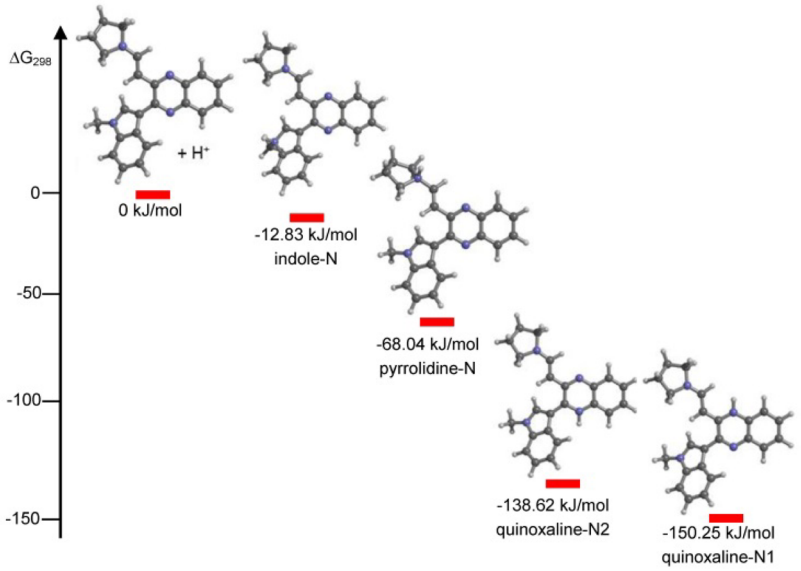

Figure 6. Thermodynamic comparison of four protonated species based on **9a** (Gaussian09 B3LYP/6-311G(d,p) PCM model for the solvent acetonitrile).

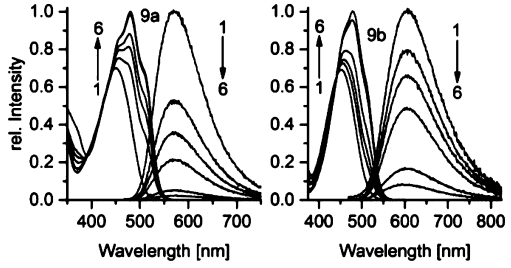

Figure 7. Spectroscopic study of the protonation of the dyes **9a** (left) and **9d** (right) in a DMSO-water mixture. The concentration of the dyes was 2 μM. The absorption (550 nm and below) and emission (500 nm upward) is shown by different concentrations of hydrochloric acid (1:0 mM; 2:0.05 mM; 3:0.1 mM; 4:0.2 mM; 5:1 mM; 6:2.5 mM). Excitation was always at the isosbestic point.

approach allowed the straightforward construction of a substance library for first structure−property relationship studies. 3-Aminovinylquinoxalines were found to be highly fluorescent in organic solvents and mixtures of organic solvents and water. Moreover, they display solvatochromicity and protochromicity, underlining the charge transfer character of their absorption and emission, and reveal hydrogen bonding- and protonation-induced fluorescence quenching. The detailed photophysical studies were corroborated with computations to rationalize the electronic structure and the underlying electronic transitions responsible for the spectroscopic effects. Furthermore, as found only recently, all four dyes additionally display a strong emission in the solid state which we are currently studying in more detail, together with the aggregation behavior of these dyes in mixtures of organic solvents and water and the occurrence of aggregation-induced emission enhancement (AIEE).

EXPERIMENTAL SECTION

General Considerations. Reagents and solvents were purchased reagent grade and used without further purification. The reaction progress was observed qualitatively using TLC silica gel 60 F254 aluminum sheets. The spots were detected with UV light at 254 and 365 nm and with aqueous potassium permanganate solution. Chemical shifts δ in the ^{1}H NMR and ^{13}C NMR spectra are reported in ppm relative to $CDCl_3$. The assignments of quaternary C, CH, CH_2, and CH_3 signals were made by using DEPT spectra.

Spectroscopic Measurements. IR spectra were recorded with neat compounds under attenuated total reflection (ATR) and the intensities were characterized as strong (s), middle (m), and weak (w). Absorption spectra were measured with a calibrated spectrophotometer. Emission and excitation spectra were obtained with a calibrated spectrofluorometer equipped with polarizers in the excitation and emission channel and were corrected for the wavelength dependence of the spectral responsivity of the detection channel (emission spectra; fluorescence quantum yields) or for the spectral photon flux of the excitation channel (excitation spectra).[50] The fluorescence quantum yields of the dyes were determined from spectrally corrected integrated emission spectra (on an energy scale) relative to Coumarin 153 (ϕ = 54.1% in ethanol)[51] using a previously described procedure (excitation and emission polarizer set to magic angle conditions), thereby also considering the refractive indices of the solvents of the dyes **9a**−**9d** and the reference dyes.[52] The fluorescence lifetimes were measured with a spectrofluorometer using a pulsed excitation light source (fs fianium laser-monochromator ensemble).

Procedure for the Synthesis of 2-Ethynyl-3-(1-methyl-1*H*-indol-3-yl)quinoxaline (7a). The TMS-protected ethynylquinoxaline **6a**[21] (2.31 g, 6.49 mmol) was placed in a round flask and dissolved in tetrahydrofuran (1 mL/mmol) and methanol (2 mL/mmol). Then, 2.0 equivs of potassium fluoride (766 mg, 13.0 mmol) were added. After 60 min the reaction was terminated by addition of water (10 mL), the phases were separated and the aqueous phase was extracted with dichloromethane. The combined organic layers were dried with anhydrous sodium sulfate. Thereafter, the solvents were removed in vacuo to obtain the analytically pure product **7a** in quantitative yield (1.86 g, 100%).

Yellow solid, 128 °C. ^{1}H NMR ($CDCl_3$, 300 MHz): δ 3.57 (s, 1 H), 3.90 (s, 3 H), 7.28−7.45 (m, 3 H), 7.66 (ddd, J = 8.3 Hz, J = 6.9 Hz, J = 1.5 Hz, 1 H), 7.74 (ddd, J = 8.4 Hz, J = 7.0 Hz, J = 1.5 Hz, 1 H), 8.03 (dd, J = 8.2 Hz, J = 1.2 Hz, 1 H), 8.12 (dd, J = 8.3 Hz, J = 1.2 Hz, 1 H), 8.48 (s, 1 H), 8.76−8.82 (m, 1 H). ^{13}C NMR ($CDCl_3$, 75 MHz): δ 33.4 (CH_3), 82.3 (CH), 83.4 (C_{quat}), 109.4 (CH), 111.8 (C_{quat}), 121.4 (CH), 123.0 (2 CH), 127.4 (C_{quat}), 128.6 (CH), 128.8 (CH), 130.8 (CH), 132.5 (CH), 135.5 (C_{quat}), 137.3 (C_{quat}) 139.1 (C_{quat}), 141.3 (C_{quat}), 150.3 (C_{quat}). EI + MS (m/z (%)): 284 (20), 283 (M^+, 100), 282 (57), 232 ($C_{16}H_{14}N_2^+$, 4), 231 (11), 156 (11), 155 (14), 149 (15). IR: $\tilde{\nu}$ 3267 (w), 3173 (w), 3051 (w), 2926 (w), 2091 (w), 1533 (s), 1477 (m), 1452 (m), 1422 (w), 1371 (m), 1337 (w), 1281 (w), 1240 (m), 1215 (m), 1192 (w), 1159 (w), 1121 (m), 1082 (m), 1051 (w), 1015 (w), 937 (m), 901

DOI: 10.1021/acs.joc.6b02581
J. Org. Chem. 2017, 82, 567−578

Table 6. Experimental Details of the One-Pot Four-Step Synthesis of 3-Aminovinylquinoxalines 9 (GP1 and GP2)

entry	starting material **1** or **2**	1,2-diamino arene **5**	secondary amine **8**	3-aminovinylquinoxaline **9** (yield)
1[a]	268 mg (2.00 mmol) of 1-methylindole (**1a**)	216 mg (2.00 mmol) of *ortho*-phenylenediamine (**5a**)	0.96 mL (12.0 mmol) of pyrrolidine (**8a**)	522 mg (73%) of **9a**[b]
2[a]	164 mg (2.00 mmol) of 1-methyl pyrrole (**1b**)	216 mg (2.00 mmol) of **5a**	0.96 mL (12.0 mmol) of **8a**	452 mg (74%) of **9b**[b]
3[a]	231 mg (2.00 mmol) of 2-methoxy thiophene (**1c**)	216 mg (2.00 mmol) of **5a**	0.96 mL (12.0 mmol) of **8a**	402 mg (60%) of **9c**[b]
4[c]	306 mg (2.00 mmol) of phenyl glyoxylic acid (**2a**)	216 mg (2.00 mmol) of **5a**	0.96 mL (12.0 mmol) of **8a**	342 mg (57%) of **9d**[b]
5[c]	319 mg (2.00 mmol) of 2-thiophene glyoxylic acid (**2b**)	216 mg (2.00 mmol) of **5a**	0.96 mL (12.0 mmol) of **8a**	452 mg (69%) of **9e**[b]
6[a]	268 mg (2.00 mmol) of (**1a**)	361 mg (2.00 mmol) of 1,2-diamino 4,5-dichloro benzene (**5b**)	0.96 mL (12.0 mmol) of **8a**	578 mg (68%) of **9f**[d]
7[c]	306 mg (2.00 mmol) of (**2a**)	361 mg (2.00 mmol) of **5b**	0.96 mL (12.0 mmol) of **8a**	382 mg (52%) of **9g**[d]
8[c]	319 mg (2.00 mmol) of (**2b**)	361 mg (2.00 mmol) of **5b**	0.96 mL (12.0 mmol) of **8a**	486 mg (65%) of **9h**[b]
9[c]	319 mg (2.00 mmol) of (**2b**)	326 mg (2.00 mmol) of 2,3-diamino naphthalene (**5c**)	0.96 mL (12.0 mmol) of **8a**	439 mg (61%) of **9i**[b]
10[c]	306 mg (2.00 mmol) of (**2a**)	216 mg (2.00 mmol) of **5a**	1.20 mL (12.0 mmol) of piperidine (**8b**)	270 mg (46%) of **9j**[e]

[a]According to GP1. [b]Reaction conditions for the amine addition step: 1 h, rt. [c]According to GP2. [d]Reaction conditions for the amine addition step: 1 h, 50 °C. [e]Reaction conditions for the amine addition step: 2 h, 50 °C.

(w), 737 (s), 640 (m), 613 (m) [cm^{-1}]. Anal. Calcd for $C_{19}H_{13}N_3$ (283.3): C 80.54, H 4.62, N 14.81. Found: C 80.37, H 4.49, N 14.63.

Procedures for the Synthesis of 3-Aminovinylquinoxalines 9. *From Terminal Ethynylquinoxaline **7a**.* Terminal ethynylquinoxaline **7a** (142 mg, 0.50 mmol) was placed in a reaction vessel with screw cap and dissolved in tetrahydrofuran (1.25 mL, 2.5 mL/mmol) and 0.5 mL methanol (1.0 mL/mmol). Then, 2.0 equivs pyrrolidine (8a) (0.08 mL, 1.00 mmol) were added and the reaction mixture was stirred at room temp for 1 h. Overlayering the reaction mixture with *n*-pentane led to precipitation of product **9a** at −18 °C (ice box of the refrigerator). Filtration and washing with *n*-pentane gave the analytically pure product in 75% yield (133 mg, 0.375 mmol).

*From TMS-Protected Ethynylquinoxaline **4a**.* TMS-protected ethynylquinoxaline **6a** (711 mg, 2.00 mmol) was placed in a reaction vessel with screw cap and dissolved in tetrahydrofuran (4.00 mL, 2.00 mL/mmol) and methanol (2.00 mL, 1.00 mL/mmol). Then, 2.05 equivs of pyrrolidine (**8a**) (0.33 mL, 4.10 mmol) were added and the reaction mixture was stirred for at room temp for 1 h. Overlayering the reaction mixture with *n*-pentane led to precipitation of the product **9a** at −18 °C. Filtration and washing with *n*-pentane gave the analytically pure product in 83% yield (589 mg, 1.66 mmol).

*General Procedure for the Five-Component Synthesis of 3-Aminovinylquinoxalines **9a–c, 9f** (GP1).* The π-nucleophile **1** (2.00 mmol) in dry THF (5 mL) was placed in a sintered screw-cap Schlenk tube under nitrogen atmosphere, degassed with nitrogen, and cooled to 0 °C (water/ice, 5 min) (for experimental details, see Table 6). Then, oxalyl chloride (0.18 mL, 2.00 mmol, 1.0 equiv) was added dropwise to the reaction mixture at 0 °C over the course of 1 min. The mixture was first warmed to room temp (water bath, 5 min), and then stirred at 50 °C (oil bath) for 1 h. Thereafter, the mixture was cooled to room temp (water bath, 5 min). Then, CuI (20 mg, 0.1 mmol, 5 mol%), trimethylsilyl acetylene (**3a**) (0.28 mL, 2.00 mmol, 1.0 equiv), and dry triethylamine (0.59 mL, 4.20 mmol, 2.1 equivs) were successively added to the reaction mixture, and stirring at room temperature was continued for 6 h. Then, methanol (2 mL), 1,2-diaminoarene **5** (2.00 mmol, 1.0 equiv), and acetic acid (0.23 mL, 4.00 mmol, 2.0 equivs) were successively added and the mixture was stirred at 50 °C for 1 h. Then, the cyclic secondary amine **8** (12.0 mmol, 6.0 equivs) was added and the reaction mixture was stirred at room temp to 50 °C to complete conversion. The solvents were removed in vacuo, the remaining solid was dissolved in dichloromethane and filtered through a plug of basic aluminum oxide to give the products **9**.

*General Procedure for the Four-Component Synthesis of 3-Aminovinylquinoxalines **9d,e,g–j** (GP2).* The glyoxylic acid **2** (2.00 mmol) in dry 1,4-dioxane (5 mL) was placed in a sintered screw-cap Schlenk tube under nitrogen atmosphere and degassed with nitrogen (for experimental details, see Table 6). Then, oxalyl chloride (0.18 mL, 2.00 mmol, 1.0 equiv) was added dropwise to the reaction mixture over the course of 1 min. The mixture was first stirred at room temp (water bath, 5 min), and then stirred at 50 °C (oil bath) for 4 h. Thereafter, the mixture was cooled to room temp (water bath, 5 min). Then, CuI (20 mg, 0.1 mmol, 5 mol%), trimethylsilyl acetylene (**2b**) (0.28 mL, 2.00 mmol, 1.0 equiv), and dry triethylamine (0.59 mL, 4.20 mmol, 2.1 equivs) were successively added to the reaction mixture, and stirring at room temperature was continued for 15 h. Then, methanol (2 mL), 1,2-diaminoarene **5** (2.00 mmol, 1.0 equiv), and acetic acid (0.23 mL, 4.00 mmol, 2.0 equivs) were successively added and the mixture was stirred at 50 °C for 1 h. Then, the cyclic secondary amine **8** (12.0 mmol, 6.0 equivs) was added and the reaction mixture was stirred at room temp to 50 °C to complete conversion. The solvents were removed in vacuo, the remaining solid was dissolved in dichloromethane and filtered through a plug of basic aluminum oxide to give the products **9**.

*(E)-2-(1-Methyl-1H-indol-3-yl)-3-(2-(pyrrolidin-1-yl)vinyl)-quinoxaline (**9a**).* Orange solid (522 mg, 73%), mp 184 °C. ^{1}H NMR ($CDCl_3$, 600 MHz): δ 1.83–1.93 (m, 4 H), 3.27 (br, 4 H), 3.87 (s, 3 H), 5.62 (d, J = 12.8 Hz, 1 H), 7.14–7.24 (m, 1 H), 7.24–7.33 (m, 1 H), 7.35–7.46 (m, 2 H), 7.50–7.58 (m, 1 H), 7.63 (s, 1 H), 7.78–7.84 (m, 1 H), 7.93 (d, J = 8.2 Hz, 2 H), 8.15 (d, J = 12.7 Hz, 1 H). ^{13}C NMR ($CDCl_3$, 75 MHz): δ 25.2 (CH_2), 33.0 (CH_3), 49.2 (CH_2), 94.0 (CH), 109.4 (CH), 114.6 (C_{quat}), 120.0 (CH), 122.0 (CH), 122.1 (CH), 125.6 (CH), 126.9 (CH), 127.1 (C_{quat}), 128.4 (CH), 128.5 (CH), 130.2 (CH), 137.1 (C_{quat}), 139.5 (C_{quat}), 141.3 (C_{quat}), 142.9 (CH), 148.8 (C_{quat}), 152.9 (C_{quat}). EI + MS (m/z (%)): 355 (10), 354 (M^+, 38), 353 (14), 286 (20), 285 (100), 284 ([M-C_4H_8N]$^+$, 74), 283 (21), 271 (14), 270 (15), 269 ([M-C_4H_8N−CH_3]$^+$, 12). IR: $\tilde{\nu}$ 3051 (w), 2955 (w), 2930 (w), 2866 (w), 2851 (w), 1611 (m), 1537 (m), 1506 (m), 1483 (w), 1470 (w), 1456 (m), 1423 (w), 1383 (w), 1366 (m), 1339 (m), 1310 (m), 1275 (m), 1221 (m), 1184 (w), 1148 (w), 1117 (m), 1084 (m), 1030 (w), 1013 (m), 964 (m), 949 (m), 931 (m), 908 (w), 876 (w), 841 (w), 808 (w), 756 (m), 733 (s), 667 (w), 637 (w), 610 (m) [cm^{-1}]. Anal. Calcd for $C_{23}H_{22}N_4$ (354.5): C 77.94, H 6.26, N 15.81. Found: C 78.08, H 6.00, N 15.93.

*(E)-2-(1-Methyl-1H-pyrrol-2-yl)-3-(2-(pyrrolidin-1-yl)vinyl)-quinoxaline (**9b**).* Orange solid (452 mg, 74%), mp 113 °C. ^{1}H NMR ($CDCl_3$, 300 MHz): δ 1.86–2.02 (m, 4 H), 3.36 (br, 4 H), 3.78 (s, 3 H), 5.63 (d, J = 12.8 Hz, 1 H), 6.22 (dd, J = 3.7 Hz, J = 2.6 Hz, 1 H), 6.66 (dd, J = 3.7 Hz, J = 1.7 Hz, 1 H), 6.78 (dd, J = 2.5 Hz, J = 1.8 Hz, 1 H), 7.40 (ddd, J = 8.3 Hz, J = 6.9 Hz, J = 1.4 Hz, 1 H), 7.54 (ddd, J = 8.4 Hz, J = 6.9 Hz, J = 1.4 Hz, 1 H), 7.76 (ddd, J = 8.3 Hz, J = 1.4 Hz, J = 0.5 Hz, 1 H), 7.85 (ddd, J = 8.1 Hz, J = 1.4 Hz, J = 0.4 Hz, 1 H), 8.08 (d, J = 12.8 Hz, 1

DOI: 10.1021/acs.joc.6b02581
J. Org. Chem. 2017, 82, 567–578

H). ^{13}C NMR ($CDCl_3$, 75 MHz): δ 25.2 (CH_2), 35.5 (CH_3), 49.2 (CH_2), 93.0 (CH), 107.4 (CH), 112.3 (CH), 125.0 (CH), 125.6 (CH), 127.0 (CH), 128.5 (CH), 129.0 (CH), 130.1 (C_{quat}), 138.9 (C_{quat}), 141.2 (C_{quat}), 143.2 (CH), 146.1 (C_{quat}), 153.2 (C_{quat}). EI + MS (m/z (%)): 304 (M^+, 35), 262 (12), 235 (20), 234 ([M-C_4H_8N]$^+$, 100), 233 (39), 232 (60), 221 ([M-C_5H_9N]$^+$, 19), 220 (19), 219 (11), 130 (22), 117 (13). IR (solid): $\tilde{\nu}$ 2974 (w), 2945 (w), 2847 (w), 2357 (w), 1611 (s), 1603 (m), 1539 (m), 1510 (s), 1472 (m), 1456 (m), 1443 (m), 1423 (w), 1375 (s), 1364 (m), 1333 (m), 1312 (m), 1279 (s), 1246 (m), 1227 (m), 1211 (w); 1155 (w), 1130 (m), 1115 (m), 1090 (w), 1059 (m), 1034 (w), 1013 (w), 984 (m), 966 (m), 939 (m), 872 (m), 812 (w), 783 (m), 752 (s), 723 (s), 696 (m), 665 (m), 608 (m) [cm^{-1}]. Anal. Calcd for $C_{19}H_{20}N_4$ (304.4): C 74.97, H 6.62, N 18.41. Found C 74.77, H 6.58, N 18.25.

*(E)-2-(5-Methoxythiophen-2-yl)-3-(2-(pyrrolidin-1-yl)vinyl)-quinoxaline (**9c**).* Red solid (402 mg, 60%), mp 134 °C. ^{1}H NMR ($CDCl_3$, 300 MHz): δ 1.91−2.04 (m, 4 H), 3.42 (br, 4 H), 3.97 (s, 3 H), 5.77 (d, J = 12.6 Hz, 1 H), 6.25 (d, J = 4.1 Hz, 1 H), 7.39 (ddd, J = 8.3 Hz, J = 6.9 Hz, J = 1.5 Hz, 1 H), 7.50 (d, J = 4.2 Hz, 1 H), 7.46−7.54 (m, 1 H), 7.70−75 (m, 1 H), 7.82 (dd, J = 8.2 Hz, J = 1.1 Hz, 1 H), 8.12 (d, J = 12.6 Hz, 1 H). ^{13}C NMR ($CDCl_3$, 75 MHz): δ 25.3 (CH_2), 49.4 (CH_2), 60.2 (CH_3), 93.1 (CH), 104.7 (CH), 126.0 (CH), 126.8 (CH), 126.9 (CH), 128.2 (CH), 128.7 (CH), 129.5 (C_{quat}), 139.0 (C_{quat}), 141.0 (C_{quat}), 143.5 (CH), 146.2 (C_{quat}), 151.0 (C_{quat}), 169.0 (C_{quat}). EI + MS (m/z (%)): 337 (M^+, 7), 263 (20), 262 ([M-C_2H_3OS]$^+$, 100), 252 (10), 225 (11). IR: $\tilde{\nu}$ 3096 (w), 3057 (w), 2968 (w), 2932 (w), 2859 (w), 1614 (m), 1601 (m), 1547 (w), 1506 (m), 1491 (s), 1474 (m), 1458 (m), 1425 (s), 1377 (m), 1362 (m), 1341 (m), 1306 (m), 1277 (s), 1256 (m), 1244 (w), 1209 (s); 1184 (w), 1153 (m), 1130 (m), 1113 (m), 1061 (m), 1015 (w), 991 (w), 943 (m), 930 (m), 903 (w), 874 (w), 860 (w), 827 (w), 768 (m), 746 (s), 733 (m), 719 (m), 662 (w), 625 (w), 608 (m) [cm^{-1}]. Anal. Calcd for: $C_{19}H_{19}N_3OS$ (337.4): C 67.63, H 5.68, N 12.45, S 9.50. Found: C 67.67, H 5.71, N 12.32, S 9.45.

*(E)-2-Phenyl-3-(2-(pyrrolidin-1-yl)vinyl)quinoxaline (**9d**).* Orange solid (342 mg, 57%), mp 150 °C. ^{1}H NMR ($CDCl_3$, 300 MHz): δ 1.83−1.95 (m, 4 H), 3.29 (br, 4 H), 5.27 (d, J = 12.7 Hz, 1 H), 7.37−7.53 (m, 4 H), 7.37 (ddd, J = 8.4 Hz, J = 6.9 Hz, J = 1.5 Hz, 1 H), 7.65−7.73 (m, 2 H), 7.80 (dd, J = 8.4 Hz, J = 1.0 Hz, 1 H), 7.92 (dd, J = 8.3 Hz, J = 1.2 Hz, 1 H), 8.09 (d, J = 12.7 Hz, 1 H). ^{13}C NMR ($CDCl_3$, 75 MHz): δ 25.2 (CH_2), 49.2 (CH_2), 93.2 (CH), 125.8 (CH), 127.0 (CH), 128.3 (CH), 128.5 (CH), 128.9 (CH), 129.0 (CH), 129.2 (CH), 139.2 (C_{quat}), 139.6 (C_{quat}), 142.7 (C_{quat}), 142.9 (CH), 152.3 (C_{quat}), 153.4 (C_{quat}). EI + MS (m/z (%)): 301 (M^+, 48), 300 (12), 232 (45), 231 ([M-C_4H_8N]$^+$, 100), 224 (29), 219 (12), 218 ([M-C_5H_8N]$^+$, 30), 149 (17), 116 (13), 96 (16), 84 (10), 83 (11), 77 (13), 72 (28), 71 (33), 70 (10), 57 (16), 56 (12), 55 (10). IR: $\tilde{\nu}$ 3057 (w), 2957 (w), 2853 (w), 1612 (m), 1522 (m), 1497 (w), 1475 (m), 1456 (w), 1441 (w), 1379 (m), 1364 (m), 1335 (m), 1298 (m), 1277 (m), 1252 (m), 1221 (w); 1179 (w), 1150 (m), 1113 (m), 1076 (w), 1034 (w), 1015 (m), 957 (m), 907 (w), 874 (w), 843 (w), 810 (w), 762 (s), 733 (w), 696 (s), 687 (m), 658 (w), 608 (m) [cm^{-1}]. Anal. Calcd for: $C_{20}H_{19}N_3$ (301.2): C 79.70, H 6.35, N 13.94. Found: C 79.91, H 6.45, N 13.82.

*(E)-2-(2-(Pyrrolidin-1-yl)vinyl)-3-(thiophen-2-yl)quinoxaline (**9e**).* Red solid (452 mg, 69%), mp 135 °C. ^{1}H NMR ($CDCl_3$, 300 MHz): δ 1.83−2.09 (m, 4 H), 3.24−3.60 (br, 4 H), 5.75 (d, J = 12.6 Hz, 1 H), 7.15 (dd, J = 5.1 Hz, J = 3.6 Hz, 1 H), 7.42 (ddd, J = 8.3 Hz, J = 6.9 Hz, J = 1.4 Hz, 1 H), 7.48 (dd, J = 5.1 Hz, J = 1.0 Hz, 1 H), 7.55 (ddd, J = 8.4, Hz, J = 6.9 Hz, J = 1.5 Hz, 1 H), 7.73 (dd, J = 3.7 Hz, J = 1.1 Hz, 1 H), 7.75−7.84 (br, 1 H), 7.84−7.93 (m, 1 H), 8.17 (d, J = 12.6 Hz, 1 H). ^{13}C NMR ($CDCl_3$, 75 MHz): δ 25.3 (CH_2), 48.5−50.2 (CH_2), 92.8 (CH), 126.0 (CH), 126.8 (CH), 127.3 (CH), 127.9 (CH), 128.1 (CH), 128.7 (CH), 129.4 (CH), 139.0 (C_{quat}), 141.4 (C_{quat}), 142.8 (C_{quat}), 143.8 (CH), 146.4 (C_{quat}), 151.5 (C_{quat}). EI + MS (m/z (%)): 308 (15), 307 (M^+, 70), 306 (16), 274 (15), 262 (11), 239 (13), 238 (52), 237 ([M-C_4H_8N]$^+$, 100), 224 ([M-C_5H_9N]$^+$, 22), 205 (11). IR: $\tilde{\nu}$ 3073 (w), 2963 (w), 1612 (s), 1599 (s), 1509 (s), 1504 (s), 1476 (m), 1452 (m), 1425 (m), 1377 (s), 1360 (m), 1341 (m), 1331 (m), 1288 (m), 1277 (s), 1219 (m), 1152 (m), 1111 (m), 1072 (m), 1015 (m), 957 (m), 937(w), 761 (s), 750 (s), 738 (s), 710 (s), 608 (s) [cm^{-1}]. Anal. Calcd for: $C_{18}H_{17}N_3S$ (307.4): C 70.35, H 5.57, N 13.67, S 10.43. Found: C 70.23, H 5.63, N 13.47, S 10.37.

*(E)-6,7-Dichloro-2-(1-methyl-1H-indol-3-yl)-3-(2-(pyrrolidin-1-yl)-vinyl)quinoxaline (**9f**).* Red solid (578 mg, 68%), mp 156 °C. ^{1}H NMR ($CDCl_3$, 300 MHz): δ1.82−2.01 (m, 4 H), 3.30 (br, 4 H), 3.88 (s, 3 H), 5.61 (d, J = 12.6 Hz, 1 H), 7.21 (ddd, J = 8.0 Hz, J = 7.0 Hz, J = 1.2 Hz, 1 H), 7.30 (ddd, J = 8.1 Hz, J = 6.9 Hz, J = 1.2 Hz, 1 H), 7.39 (d, J = 8.1 Hz, 1 H), 7.64 (s, 1 H), 7.85 (s, 1 H), 7.97 (s, 1 H), 7.97 (d, J = 7.9 Hz, 1 H), 8.16 (d, J = 12.8 Hz, 1 H). ^{13}C NMR ($CDCl_3$, 75 MHz): δ 25.2 (CH_2), 33.1 (CH_3), 48.0−50.28 (br, CH_2), 93.7 (CH), 109.5 (CH), 114.0 (C_{quat}), 120.3 (CH), 122.0 (CH), 122.4 (CH), 127.0 (C_{quat}), 127.4 (CH), 128.7 (C_{quat}), 129.0 (CH), 130.6 (CH), 132.0 (C_{quat}), 137.2 (C_{quat}), 138.3 (C_{quat}), 140.2 (C_{quat}), 144.0 (CH), 150.0 (C_{quat}), 153.6 (C_{quat}). EI + MS (m/z (%)): 424 (M^+{^{37}Cl, ^{35}Cl}, 10), 422 (M^+{^{35}Cl, ^{35}Cl}, 15), 357 (10), 356 ([M{^{37}Cl, ^{37}Cl}-C_4H_8N]$^+$, 18), 355 (62), 354 ([M{^{37}Cl, ^{35}Cl}-C_4H_8N]$^+$, 57), 353 (100), 352 ([M{^{35}Cl, ^{35}Cl}-C_4H_8N]$^+$, 65), 351 (12), 340 (12), 339 ((M{^{37}Cl, ^{35}Cl}-C_4H_8N−CH_3)$^+$, 18), 338 (14), 337 ([M{^{35}Cl, ^{35}Cl}-C_4H_8N−CH_3]$^+$, 12), 169 (11), 206 (14), 156 (12), 155 (15). IR: $\tilde{\nu}$ 2976 (w), 2953 (w), 2927 (w), 2903 (w), 2874 (w), 2851 (w), 1605 (m), 1530 (m), 1506 (s), 1479 (m), 1454 (m), 1427 (w), 1381 (m), 1362 (m), 1337 (m), 1306 (m), 1279 (m), 1258 (m), 1238 (m), 1219 (w), 1209 (m), 1186 (m), 1171 (m), 1153 (m), 1101 (m), 1084 (m), 1036 (m), 1018 (w), 986 (m), 966 (m), 951 (m), 928 (m), 908 (w), 883 (s), 808 (w), 750 (m), 739 (s), 673 (m), 654 (m) [cm^{-1}]. Anal. Calcd for $C_{23}H_{20}Cl_2N_4$ (423.3): C 65.25, H 4.76, N 13.22; Found: C 65.54, H 4.59, N 13.22.

*(E)-6,7-Dichloro-2-phenyl-3-(2-(pyrrolidin-1-yl)vinyl)quinoxaline (**9g**).* Dark-red solid (382 mg, 52%), Mp 164 °C. ^{1}H NMR ($CDCl_3$, 300 MHz): δ 1.86−2.00 (m, 4 H), 3.32 (s, 4 H), 5.24 (d, J = 12.5 Hz, 1 H), 7.39−7.56 (m, 3 H), 7.59−7.74 (m, 2 H), 7.88 (s, 1 H), 7.98 (s, 1 H), 8.13 (d, J = 12.2 Hz, 1 H). ^{13}C NMR ($CDCl_3$, 75 MHz): δ 25.2 (CH_2), 47.8−50.7 (CH_2), 92.8 (CH), 127.3 (CH) 128.4 (CH), 128.85 (CH), 128.93 (CH), 129.0 (C_{quat}), 129.5 (CH), 133.3 (C_{quat}), 137.9 (C_{quat}), 138.9 (C_{quat}), 144.2 (CH), 153.0 (C_{quat}), 154.6 (C_{quat}). EI + MS (m/z (%)): 371 ([M{^{37}Cl,^{35}Cl}]$^+$, 26), 370 (16), 369 ([M{^{35}Cl,^{35}Cl}]$^+$, 39), 368 (12), 303 ([M{^{37}Cl,^{37}Cl}-C_4H_8N]$^+$, 16), 302 (35), 301 ([M-{^{37}Cl,^{35}Cl}-C_4H_8N]$^+$, 70), 300 (56), 299 ([M{^{35}Cl,^{35}Cl}-C_4H_8N]$^+$, 100), 294 ([M{^{37}Cl,^{35}Cl}-C_6H_5]$^+$, 17), 292 ([M{^{35}Cl,^{35}Cl}-C_6H_5]$^+$, 26), 288 ([M{^{37}Cl,^{35}Cl}-C_5H_9N]$^+$,16), 287 (13), 286 ([M{^{35}Cl,^{35}Cl}-C_5H_9N]$^+$, 22), 264 (18), 150 (12), 96 ($C_6H_{10}N^+$, 18), 84 (13), 70 (11). IR: $\tilde{\nu}$ 2953 (w), 2851 (w), 1609 (m), 1539 (w), 1516 (s), 1506 (s), 1495 (m), 1477 (m), 1452 (m), 1443 (m), 1416 (w), 1371 (m), 1333 (m),1312 (m), 1302 (m), 1277 (m), 1260 (m), 1244 (m), 1219 (m), 1207 (m), 1180 (w), 1146 (s), 1103 (m), 1076 (m), 1036 (m),1013 (m), 999 (m), 978 (m), 959 (m), 920 (m), 908 (w), 885 (m), 860 (m), 810 (m), 773 (m), 760 (m), 719 (m), 696 (s), 675 (m), 650 (m), 631 (m) [cm^{-1}]. Anal. Calcd for $C_{20}H_{17}Cl_2N_3$ (370.3): C 64.88, H 4.63, N 11.35; gef.: C 64.80, H 4.55, N 11.23.

*(E)-6,7-Dichloro-2-(2-(pyrrolidin-1-yl)vinyl)-3-(thiophen-2-yl)-quinoxaline (**9h**).* Red solid (486 mg, 65%), mp 163 °C. ^{1}H NMR ($CDCl_3$, 300 MHz): δ 1.85−2.08 (m, 4 H), 3.41 (br, 4 H), 5.71 (d, J = 12.5 Hz, 1 H), 7.14 (dd, J = 5.1 Hz, J = 3.7 Hz, 1 H), 7.49 (dd, J = 5.1 Hz, J = 1.1 Hz, 1 H), 7.74 (dd, J = 3.7 Hz, J = 1.1 Hz, 1 H), 7.81 (s, 1 H), 7.94 (s, 1 H), 8.15 (d, J = 12.5 Hz, 1 H). ^{13}C NMR ($CDCl_3$, 75 MHz): δ 25.3 (CH_2), 47.0−53.0 (CH_2), 92.5 (CH), 127.3 (CH), 127.4 (CH), 128.4 (CH), 128.5 (CH), 129.1 (CH), 129.2 (C_{quat}), 133.1 (C_{quat}), 137.7 (C_{quat}), 140.5 (C_{quat}), 142.5 (C_{quat}), 144.6 (CH), 147.3 (C_{quat}), 152.3 (C_{quat}). EI + MS (m/z (%)): 378 (10), 377 (M^+{^{37}Cl, ^{35}Cl}$^+$, 44), 376 (21), 375 (M^+{^{35}Cl, ^{35}Cl}$^+$, 61), 374 (13), 344 (10), 342 (16), 309 ([M{^{37}Cl, ^{37}Cl}-C_4H_8N]$^+$, 21), 308 (44), 307 ([M{^{37}Cl, ^{35}Cl}-C_4H_8N]$^+$, 80), 306 (68), 305 ([M{^{35}Cl, ^{35}Cl}-C_4H_8N]$^+$, 100), 294 ([M{^{37}Cl, ^{35}Cl}-C_5H_9N]$^+$, 15), 292 ([M{^{35}C, ^{35}Cl}-C_5H_9N]$^+$, 21), 273 (13), 269 (11), 153 (10), 96 ($C_6H_{10}N^+$, 16), 70 ($C_4H_8N^+$, 18). IR: $\tilde{\nu}$ 2967 (w), 2853 (w), 1609 (s), 1508 (s), 1504 (s), 1474 (m), 1454 (s), 1433 (m), 1371 (s), 1364 (s), 1338 (m), 1327 (m), 1312 (m), 1281 (s), 1260 (m), 1234 (s), 1219 (s), 1198 (m), 1138 (s), 1113 (s), 1105 (s), 1084 (m), 1059 (m), 984 (m), 962 (m), 908 (w), 883 (m), 872 (s), 856 (m), 849 (m), 802 (w), 777 (w), 762 (m), 731 (s), 723 (s), 702 (m), 679 (w), 652 (w) [cm^{-1}]. HR-MS (ESI) calcd. for $C_{18}H_{15}{}^{35}Cl_2N_3S$+H$^+$: 376.0437; Found: 376.0438.

DOI: 10.1021/acs.joc.6b02581
J. Org. Chem. 2017, 82, 567−578

*(E)-2-(2-(Pyrrolidin-1-yl)vinyl)-3-(thiophen-2-yl)benzo[g]-quinoxaline (**9i**).* Violet solid (439 mg, 61%), mp 150 °C. ^{1}H NMR ($CDCl_3$, 300 MHz): δ 1.90−2.05 (m, 4 H), 3.42 (br, 4 H), 5.79 (d, J = 12.5 Hz, 1 H), 7.17 (dd, J = 5.1 Hz, J = 3.7 Hz, 1 H), 7.34−49 (m, 2 H), 7.51 (dd, J = 5.1 Hz, J = 1.1 Hz, 1 H), 7.79 (dd, J = 3.7 Hz, J = 1.1 Hz, 1 H), 7.92−8.00 (m, 2 H), 8.24 (2, 1 H), 8.27 (d, J = 12.5 Hz, 1 H), 8.43 (s, 1 H). ^{13}C NMR ($CDCl_3$, 75 MHz): δ 25.3 (CH_2), 47.7−50.7 (CH_2), 93.3 (CH), 123.3 (CH), 124.8 (CH), 126.1 (CH), 126.8 (CH), 127.3 (CH), 127.8 (CH), 128.3 (CH), 128.4 (CH), 128.6 (CH), 131.9 (C_{quat}), 134.3 (C_{quat}), 137.0 (C_{quat}), 138.6 (C_{quat}), 142.9 (C_{quat}), 144.4 (CH), 148.6 (C_{quat}), 151.6 (C_{quat}). EI + MS (m/z (%)): 358 (15), 357 (M, 60), 356 (20), 324 (13), 312 (15), 289 (17), 288 (64), ([M-C_4H_8N]$^+$, 81), 278 (11), 276 (23), 275 (18), 274 ([M-C_5H_9N]$^+$, 28), 262 (36), 255 (11), 250 (11), 179 (14), 127 (14), 126 (60), 88 (100), 43 (11). IR: $\tilde{\nu}$ 2969 (w), 2864 (w), 1672 (w), 1600 (s), 1528 (m), 1514 (s), 1499 (s), 1474 (m), 1454 (m), 1422 (m), 1396 (s), 1364 (s), 1354 (s), 1341 (s), 1315 (m), 1272 (s), 1261 (s), 1242 (s), 1225 (m), 1148 (s), 1130 (m), 1109 (s), 1080 (m), 1045 (m), 972 (m), 916 (m), 873 (s), 864 (s), 852 (m), 802 (m), 770 (m), 735 (s), 708 (s), 604 (m) [cm^{-1}]. Anal. Calcd for: $C_{22}H_{19}N_3S$ (357.5): C 73.92, H 5.36, N 11.75, S 8.97. Found: C 73.86, H 5.50, N 11.79, S 8.92.

*(E)-2-Phenyl-3-(2-(piperidin-1-yl)vinyl)quinoxaline (**9j**).* Red-brown solid (270 mg, 46%), mp 184 °C. ^{1}H NMR ($CDCl_3$, 300 MHz): δ 1.60 (s, 6 H), 3.21 (br, 4 H), 5.44 (d, J = 12.9 Hz, 1 H), 7.41−7.53 (m, 4 H), 7.58 (ddd, J = 8.4 Hz, J = 6.9 Hz, J = 1.5 Hz, 1 H), 7.62−7.73 (m, 2 H), 7.77−7.92 (m, 2 H), 7.91 (dd, J = 8.2 Hz, J = 1.4 Hz, J = 0.6 Hz, 1 H). ^{13}C NMR ($CDCl_3$, 75 MHz): δ 24.1 (CH_2), 25.4 (CH_2), 49.8 (CH_2), 92.2 (CH), 126.0 (CH), 127.1 (CH), 128.4 (CH), 128.5 (CH), 128.9 (CH), 129.1 (CH), 129.3 (CH), 139.5 (C_{quat}), 142.0 (C_{quat}), 146.6 (CH), 152.4 (C_{quat}), 153.5 (C_{quat}). EI + MS (m/z (%)): 316 (17), 315 (M$^+$, 72), 314 (24), 239 (12), 238 ([M-C_6H_5]$^+$, 73), 231 ([M-$C_5H_{10}N$]$^+$, 100), 219 (17), 218 ([M-$C_6H_{11}N$]$^+$, 21), 120 (11). IR: $\tilde{\nu}$ 3055 (w), 2940 (w), 2920 (w), 2851 (w), 1607 (s), 1574 (m), 1520 (s), 1506 (m), 1493 (m), 1441 (m), 1385 (s), 1368 (m), 1325 (m), 1287 (m), 1279 (m), 1244 (s), 1200 (m), 1165 (m), 1155 (m), 1109 (s), 1074 (m), 1030 (m), 997 (m), 974 (m), 937 (m), 920 (m), 905 (m), 883 (w), 853 (m), 766 (m), 750 (s), 735 (m), 700 (s), 684 (m), 667 (m), 621 (s) [cm^{-1}]. Anal. Calcd for $C_{21}H_{21}N_3$ (315.4): C 79.97, H 6.71, N 13.32; Found: C 80.17, H 6.62, N 13.16.

*Protonation of **9a**.* 3-Aminovinyl quinoxaline **9a** (177 mg, 0.50 mmol) was placed in a reaction vessel with screw cap and dissolved in tetrahydrofuran (1.25 mL) and methanol (0.5 mL). Then, hydrochloric acid (1 mL, 37%, 12.1 mmol) was added to give a dark violet suspension and the reaction mixture was stirred for 1 h at room temp. Thereafter, a red precipitate formed upon the addition of 10 mL of water. The solid was extracted with dichloromethane. The combined organic layers were dried with anhydrous sodium sulfate and the solvents was removed in vacuo to give compound **9a-H**$^+$ (0.193 mg, 98%).

*(E)-2-(1-Methyl-1H-indol-3-yl)-3-(2-(pyrrolidin-1-yl)vinyl)-quinoxaline·hydrochloride (**9a-H**$^+$).* Red solid (0.193 mg, 98%), mp 193 °C. ^{1}H NMR ($CDCl_3$, 600 MHz): δ 1.95−2.01 (br, 4 H), 3.18 (t, J = 5.9 Hz, 2 H), 3.92 (s, 3 H), 3.95 (t, J = 6.0 Hz, 2 H), 5.68 (d, J = 12.6 Hz, 1 H), 7.24 (t, J = 7.2 Hz, 1 H), 7.33 (t, J = 7.6 Hz, 1 H), 7.42 (t, J = 8.4 Hz, 1 H), 7.45 (ddd, J = 8.2 Hz, J = 7.2 Hz, J = 1.1 Hz, 1 H), 7.45 (ddd, J = 8.4 Hz, J = 7.2 Hz, J = 1.1 Hz, 1 H), 7.70 (s, 1 H), 7.80 (d, J = 8.0 Hz, 1 H), 7.84 (d, J = 7.5 Hz, 1 H), 8.60 (d, J = 8.0 Hz, 1 H), 10.13 (d, J = 12.4 Hz, 1 H), 15.05 (br, 1 H). ^{13}C NMR ($CDCl_3$, 75 MHz): δ 24.7 (CH_2), 24.8 (CH_2), 33.3 (CH_3), 47.6 (CH_2), 53.9 (CH_2), 89.3 (CH), 110.0 (CH), 112.6 (C_{quat}), 118.6 (CH), 120.8 (CH), 121.5 (CH), 122.9 (CH), 126.2 (C_{quat}), 126.6 (CH), 128.4 (CH), 129.5 (C_{quat}), 131.09 (CH), 131.13 (CH), 137.2 (2 C_{quat}), 145.6 (C_{quat}), 151.9 (C_{quat}), 154.8 (C_{quat}). MALDI-MS (m/z): 355.4 [MH$^+$-Cl]. IR: $\tilde{\nu}$ 3127 (w), 3078 (w), 3034 (w), 2957 (w), 2916 (w), 2872 (w), 2673 (w), 1599 (s), 1528 (s), 1491 (m), 1476 (m), 1458 (m), 1406 (s), 1379 (m), 1364 (s), 1342 (s), 1331 (m), 1273 (s), 1261 (m); 1234 (s), 1182 (m), 1161 (m), 1128 (m), 1111 (m), 1088 (m), 1013 (w), 991 (w), 947 (m), 932 (w), 897 (m), 860 (m), 802 (w), 765 (s), 756 (s), 739 (s), 664 (w), 638 (w) [cm^{-1}]. Anal. Calcd for: $C_{23}H_{23}ClN_4 \cdot 1/3\ H_2O$ (390.9 + 6.01): C 69.60, H 6.01, N 14.12. Found: C 69.44, H 5.76, N 13.98.

■ ASSOCIATED CONTENT

Supporting Information

The Supporting Information is available free of charge on the ACS Publications website at DOI: 10.1021/acs.joc.6b02581.

Experimental details on the optimization studies; spectroscopic data and NMR spectra of compounds **7a**, **9**, and **9a-H**$^+$; Stokes shift-E_T^N-plot; computational data of compounds **9a**−**9d** and **9a-H**$^+$ (PDF)

X-ray crystallographic data of compound **9a** (CIF)

■ AUTHOR INFORMATION

Corresponding Authors

*Ute.Resch@bam.de

*ThomasJJ.Mueller@uni-duesseldorf.de

ORCID

Ute Resch-Genger: 0000-0002-0944-1115

Notes

The authors declare no competing financial interest.

■ ACKNOWLEDGMENTS

The financial support of the Deutsche Forschungsgemeinschaft DFG (Mu 1088/9-1) and the Fonds der Chemischen Industrie is gratefully acknowledged. The authors cordially thank Dr. Bernhard Mayer for experimental assistance and discussion. This work is dedicated on the occasion of the 70th birthday of Prof. Dr. Klaus Müllen.

■ REFERENCES

(1) *Functional Organic Materials*; Müller, T. J. J., Bunz, U. H. F., Eds.; Wiley-VCH: Weinheim, 2007.

(2) Forrest, S. R.; Thompson, M. E. *Chem. Rev.* **2007**, *107*, 923−924.

(3) For reviews on OFETs, see e.g. (a) Torsi, L.; Magliulo, M.; Manoli, K.; Palazzo, G. *Chem. Soc. Rev.* **2013**, *42*, 8612−8628. (b) Mas-Torrent, M.; Rovira, C. *Chem. Soc. Rev.* **2008**, *37*, 827−838. For reviews on OLEDs, see e.g. (c) Thejo Kalyani, N.; Dhoble, S. J. *Renewable Sustainable Energy Rev.* **2012**, *16*, 2696−2723. (d) Kamtekar, K. T.; Monkman, A. P.; Bryce, M. R. *Adv. Mater.* **2010**, *22*, 572−582. For a review on DSSCs, see e.g. (e) Hagfeldt, A.; Boschloo, G.; Sun, L.; Kloo, L.; Pettersson, H. *Chem. Rev.* **2010**, *110*, 6595−6663.

(4) Loving, G. S.; Sainlos, M.; Imperiali, B. *Trends Biotechnol.* **2010**, *28*, 73−83.

(5) (a) Carter, K. P.; Young, A. M.; Palmer, A. E. *Chem. Rev.* **2014**, *114*, 4564−4601. (b) Kobayashi, H.; Ogawa, M.; Alford, R.; Choyke, P. L.; Urano, Y. *Chem. Rev.* **2010**, *110*, 2620−2640.

(6) Lakowicz, J. R. *Principles of Fluorescence Spectroscopy*, 3rd ed.; Springer: Berlin/Heidelberg, 2006; pp 623−674.

(7) (a) Schäferling, M. *Angew. Chem., Int. Ed.* **2012**, *51*, 3532−3554. (b) Demchenko, A. P. *Methods Appl. Fluoresc.* **2013**, *1*, 022001. (c) Han, J. Y.; Burgess, K. *Chem. Rev.* **2010**, *110*, 2709−2728.

(8) Demchenko, A. P.; Mély, Y.; Duportail, G.; Klymchenko, A. S. *Biophys. J.* **2009**, *96*, 3461−3470.

(9) Grabowski, Z. R.; Rotkiewicz, K.; Rettig, W. *Chem. Rev.* **2003**, *103*, 3899−4031.

(10) Hantzsch, A. *Ber. Dtsch. Chem. Ges. B* **1922**, *55*, 953−979.

(11) Reichardt, C. *Chem. Rev.* **1994**, *94*, 2319−2358.

(12) Balkenhohl, F.; von dem Bussche-Hünnefeld, C.; Lansky, A.; Zechel, C. *Angew. Chem., Int. Ed. Engl.* **1996**, *35*, 2288−2337.

(13) (a) Burke, M. D.; Schreiber, S. L. *Angew. Chem., Int. Ed.* **2004**, *43*, 46−58. (b) Ruijter, E.; Scheffelaar, R.; Orru, R. V. A. *Angew. Chem., Int. Ed.* **2011**, *50*, 6234−6346.

(14) (a) Ugi, I. *J. Prakt. Chem./Chem.-Ztg.* **1997**, *339*, 499−516. (b) Weber, L.; Illgen, K.; Almstetter, M. *Synlett* **1999**, *1999*, 366−374.

(15) Müller, T. J. J. In *Relative Reactivities of Functional Groups as the Key to Multicomponent Reactions in Multicomponent Reactions 1*; Müller, T. J. J., Ed.; Georg Thieme Verlag: Stuttgart, 2014; pp 5−27.

(16) Touré, B. B.; Hall, D. G. *Chem. Rev.* **2009**, *109*, 4439−4486.
(17) (a) Huang, Y.; Yazbak, A.; Dömling, A. Multicomponent Reactions. In *Green Techniques for Organic Synthesis and Medicinal Chemistry*; Zhang, W., Cue, B. W., Eds.; John Wiley & Sons, Ltd: Chichester, UK, 2012; pp 499−522. (b) Kalinski, C.; Lemoine, H.; Schmidt, J.; Burdack, C.; Kolb, J.; Umkehrer, M.; Ross, G. *Synthesis* **2008**, *2008*, 4007−4011.
(18) (a) Müller, T. J. J.; D'Souza, D. M. *Pure Appl. Chem.* **2008**, *80*, 609−620. (b) Levi, L.; Müller, T. J. J. *Eur. J. Org. Chem.* **2016**, *2016*, 2902−2918. (c) Levi, L.; Müller, T. J. J. *Chem. Soc. Rev.* **2016**, *45*, 2825−2846.
(19) (a) Recent review on luminescent quinoxalines, see e.g. Achelle, S.; Baudequin, C.; Plé, N. *Dyes Pigm.* **2013**, *98*, 575−600. (b) Achelle, S.; Barsella, A.; Baudequin, C.; Caro, B.; Robin-le Guen, F. *J. Org. Chem.* **2012**, *77*, 4087−4096. (c) Wang, H.; Chen, G.; Liu, Y.; Hu, I.; Xu, X.; Ji, S. *Dyes Pigm.* **2009**, *83*, 269−275. (d) Thomas, K. R. J.; Lin, J. T.; Tao, Y.-T.; Chuen, C.-H. *Chem. Mater.* **2002**, *14*, 2796−2802. (e) Thomas, K. R. J.; Velusamy, M.; Lin, J. T.; Chuen, C.-H.; Tao, Y.-T. *Chem. Mater.* **2005**, *17*, 1860−1866.
(20) Wu, Y.; Zhu, W. *Chem. Soc. Rev.* **2013**, *42*, 2039−2058.
(21) Gers, C. F.; Nordmann, J.; Kumru, C.; Frank, W.; Müller, T. J. J. *J. Org. Chem.* **2014**, *79*, 3296−3310.
(22) Zhang, Z.; Dai, Z.; Jiang, X. *Asian J. Org. Chem.* **2015**, *4*, 1370−1374.
(23) Kudo, K.; Momotake, A.; Kanna, Y.; Nishimura, Y.; Arai, T. *Chem. Commun.* **2011**, *47*, 3867−3869.
(24) Kudo, K.; Momotake, A.; Tanaka, J. K.; Miwa, Y.; Arai, T. *Photochem. Photobiol. Sci.* **2012**, *11*, 674−678.
(25) (a) Chang, D. W.; Lee, H. J.; Kim, J. H.; Park, S. Y.; Park, S. M.; Dai, L.; Baek, J. B. *Org. Lett.* **2011**, *13*, 3880−3883. (b) Pei, K.; Wu, Y. Z.; Wu, W. J.; Zhang, Q.; Chen, B. Q.; Tian, H.; Zhu, W. H. *Chem. - Eur. J.* **2012**, *18*, 8190−8200.
(26) (a) Gobec, S.; Urleb, U. Quinoxalines. *Science of Synthesis* **2003**, *16*, 848−852. (b) Saifina, D. F.; Mamedov, N. A. *Russ. Chem. Rev.* **2010**, *79*, 351−370.
(27) (a) Hinsberg, O. *Ber. Dtsch. Chem. Ges.* **1884**, *17*, 318−323. (b) Körner, G. *Ber. Dtsch. Chem. Ges.* **1884**, *17*, A572−A573.
(28) (a) Patidar, A. K.; Jeyakandan, M.; Mobiya, A. K.; Selvan, G. *Int. J. Pharm. Technol. Res.* **2011**, *3*, 386−392. (b) Rong, F.; Chow, S.; Yan, S.; Larson, G.; Hong, Z.; Wu, J. *Bioorg. Med. Chem. Lett.* **2007**, *17*, 1663−1666. (c) Fray, M. J.; Bull, D. J.; Carr, C. L.; Gautier, C. L.; Mowbray, C. E.; Stobie, A. *J. Med. Chem.* **2001**, *44*, 1951−1962. (d) Seitz, L. E.; Suling, W. J.; Reynolds, R. C. *J. Med. Chem.* **2002**, *45*, 5604−5606. (e) Corona, P.; Carta, A.; Loriga, M.; Vitale, G.; Paglietti, G. *Eur. J. Med. Chem.* **2009**, *44*, 1579−1591. (f) Ginzinger, W.; Mühlgassner, G.; Arion, V. B.; Jakupec, M. A.; Roller, A.; Galanski, M.; Reithofer, M.; Berger, W.; Keppler, B. K. *J. Med. Chem.* **2012**, *55*, 3398−3413.
(29) Baumann, M.; Baxendale, I. R. *Beilstein J. Org. Chem.* **2013**, *9*, 2265−2319.
(30) (a) Glyoxylation: Merkul, E.; Dohe, J.; Gers, C.; Rominger, F.; Müller, T. J. J. *Angew. Chem., Int. Ed.* **2011**, *50*, 2966−2969. (b) Activation: Boersch, C.; Merkul, E.; Müller, T. J. J. *Angew. Chem., Int. Ed.* **2011**, *50*, 10448−10452.
(31) (a) Bowden, K.; Braude, E. A.; Jones, E. R. H.; Weedon, B. C. L. *J. Chem. Soc.* **1946**, 45−52. (b) Bohlmann, F.; Rahtz, D. *Chem. Ber.* **1957**, *90*, 2265−2272. (c) Bagley, M. C.; Glover, C.; Merritt, E. A. *Synlett* **2007**, *2007*, 2459−2482.
(32) (a) Tyaglivy, A. S.; Gulevskaya, A. V.; Pozharskii, A. F.; Askalepova, O. I. *Tetrahedron* **2013**, *69*, 9804−9812. (b) Ames, D. E.; Brohi, I. M. *J. Chem. Soc., Perkin Trans. 1* **1980**, 1384−1389.
(33) (a) Gulevskaya, A. V.; Van Dang, S.; Pozharskii, A. F. *J. Heterocycl. Chem.* **2005**, *42*, 413−419. (b) Gulevskaya, A. V.; Van Dang, S.; Tyaglivy, A. S.; Pozharskii, A. F.; Kazheva, O. N.; Chekhlov, A. N.; Dyachenko, O. A. *Tetrahedron* **2010**, *66*, 146−151. Based on pyrazine core: (c) Simpson, I.; St-Gallay, S. A.; Stokes, S.; Whittaker, D. T. E.; Wiewiora, R. *Tetrahedron Lett.* **2015**, *56*, 1492−1495.
(34) (a) Müller, T. J. J.; Robert, J. P.; Schmälzlin, E.; Bräuchle, C.; Meerholz, K. *Org. Lett.* **2000**, *2*, 2419−2422. (b) Karpov, A. S.; Rominger, F.; Müller, T. J. J. *J. Org. Chem.* **2003**, *68*, 1503−1511.
(35) Wang, H.; Chen, G.; Liu, Y.; Hu, I.; Xu, X.; Ji, S. *Dyes Pigm.* **2009**, *83*, 269−275.
(36) Wuts, P. G. M.; Greene, T. W. *Greene's protective groups in organic synthesis*, 4th ed.; John Wiley & Sons, Inc., 2007; p 928.
(37) Crystallographic data (excluding structure factors) for the structure reported in this article have been deposited with the Cambridge Crystallographic Data Centre as supplementary publication nos. CCDC-1454071 (**9a**). Copies of the data can be obtained free of charge on application to CCDC, 12 Union Road, Cambridge CB2 1EZ, UK (Fax: + 44−1223/336−033; E-mail: deposit@ccdc.cam.ac.uk).
(38) Valeur, B.; Berberan-Santos, M. N. *Molecular Fluorescence: Principles and Applications*; Wiley-VCH: Weinheim, 2001.
(39) Nad, S.; Pal, H. *J. Phys. Chem. A* **2001**, *105*, 1097−1106.
(40) Resch-Genger, U.; Li, Y. Q.; Bricks, J. L.; Kharlanov, V.; Rettig, W. *J. Phys. Chem. A* **2006**, *110*, 10956−10971.
(41) Xie, G.; Sueishi, Y.; Yamamoto, S. *J. Photochem. Photobiol., A* **2004**, *162*, 449−456.
(42) Frisch, M. J.; Trucks, G. W.; Schlegel, H. B.; Scuseria, G. E.; Robb, M. A.; Cheeseman, J. R.; Scalmani, G.; Barone, V.; Mennucci, B.; Petersson, G. A.; Nakatsuji, H.; Caricato, M.; Li, X.; Hratchian, H. P.; Izmaylov, A. F.; Bloino, J.; Zheng, G.; Sonnenberg, J. L.; Hada, M.; Ehara, M.; Toyota, K.; Fukuda, R.; Hasegawa, J.; Ishida, M.; Nakajima, T.; Honda, Y.; Kitao, O.; Nakai, H.; Vreven, T.; Montgomery, J. A., Jr.; Peralta, J. E.; Ogliaro, F.; Bearpark, M.; Heyd, J. J.; Brothers, E.; Kudin, K. N.; Staroverov, V. N.; Kobayashi, R.; Normand, J.; Raghavachari, K.; Rendell, A.; Burant, J. C.; Iyengar, S. S.; Tomasi, J.; Cossi, M.; Rega, N.; Millam, J.; Klene, M.; Knox, J. E.; Cross, J. B.; Bakken, V.; Adamo, C.; Jaramillo, J.; Gomperts, R.; Stratmann, R. E.; Yazyev, O.; Austin, A. J.; Cammi, R.; Pomelli, C.; Ochterski, J. W.; Martin, R. L.; Morokuma, K.; Zakrzewski, V. G.; Voth, G. A.; Salvador, P.; Dannenberg, J. J.; Dapprich, S.; Daniels, A. D.; Farkas, O.; Foresman, J. B.; Ortiz, J. V.; Cioslowski, J.; Fox, D. J. *Gaussian 09*, Revision A.02; Gaussian, Inc.: Wallingford, CT, 2009.
(43) (a) Lee, C.; Yang, W.; Parr, R. G. *Phys. Rev. B: Condens. Matter Mater. Phys.* **1988**, *37*, 785−789. (b) Becke, A. D. *J. Chem. Phys.* **1993**, *98*, 1372−1377. (c) Becke, A. D. *J. Chem. Phys.* **1993**, *98*, 5648−5652. (d) Kim, K.; Jordan, K. D. *J. Phys. Chem.* **1994**, *98*, 10089−10094. (e) Stephens, P. J.; Devlin, F. J.; Chabalowski, C. F.; Frisch, M. J. *J. Phys. Chem.* **1994**, *98*, 11623−11627.
(44) Krishnan, R.; Binkley, J. S.; Seeger, R.; Pople, J. A. *J. Chem. Phys.* **1980**, *72*, 650−654.
(45) Scalmani, G.; Frisch, M. J. *J. Chem. Phys.* **2010**, *132*, 114110.
(46) Yanai, T.; Tew, D.; Handy, N. *Chem. Phys. Lett.* **2004**, *393*, 51−57.
(47) (a) Berezhkovskii, A. M. *Chem. Phys.* **1992**, *164*, 331−339. (b) Cammi, R.; Tomasi, J. *Int. J. Quantum Chem.* **1995**, *56*, 465−474. (c) Mennucci, B.; Cammi, R.; Tomasi, J. *J. Chem. Phys.* **1998**, *109*, 2798−2807. (d) Li, X.-Y.; Fu, K.-X. *J. Comput. Chem.* **2004**, *25*, 500−509. (e) Cammi, R.; Corni, S.; Mennucci, B.; Tomasi, J. *J. Chem. Phys.* **2005**, *122*, 104513.
(48) Jaung, J.-Y. *Dyes Pigm.* **2006**, *71*, 245−250.
(49) Lloyd, D.; McNab, H. *Angew. Chem., Int. Ed. Engl.* **1976**, *15*, 459−468.
(50) Resch-Genger, U.; DeRose, P. C. *Pure Appl. Chem.* **2012**, *84*, 1815−1835.
(51) Würth, C.; Grabolle, M.; Pauli, J.; Spieles, M.; Resch-Genger, U. *Anal. Chem.* **2011**, *83*, 3431−3439.
(52) Würth, C.; Grabolle, M.; Pauli, J.; Spieles, M.; Resch-Genger, U. *Nat. Protoc.* **2013**, *8*, 1535−1550.

DOI: 10.1021/acs.joc.6b02581
J. Org. Chem. 2017, 82, 567−578